DEVELOPMENT OF NOVEL MULTILAYERED PARTICLES FOR DRUG DELIVERY AND CELL ISOLATION APPLICATIONS

by

Bhanuprasanth Koppolu

Presented to the Faculty of the Graduate School of

The University of Texas at Arlington in Partial Fulfillment

of the Requirements

for the Degree of

MASTER OF SCIENCE IN BIOMEDICAL ENGINEERING

THE UNIVERSITY OF TEXAS AT ARLINGTON

December 2008

ACKNOWLEDGEMENTS

I would like to thank Dr. Kytai Nguyen for giving me the opportunity to work in her laboratory for the past two years and being my advisor. Her continuous support and belief in my abilities encouraged me to complete this thesis successfully. She was also positive about my lab work motivating me to reach my goal. I appreciate her suggestion, guidance, and patience throughout my stay in her Lab.

I would also like to thank Dr. Jian Yang and Dr. Dr. Cheng-Jen Chuong for serving on my thesis committee. I would like to take this opportunity to thank Maham Rahimi and Sivani Priya Nattama who trained and guided me during my first steps in the world of nanomedicine and tissue engineering. I would like to express my deep gratitude to all my lab mates, in particular Aniket wadajkar, Jennifer Hua, Soujanya Kona, Hao Xu, Manasa Koratala and Nathassia Corzo for their continuous support in the lab.

Lastly and most importantly, I thank my parents, Mr. Bhupathinaidu Koppolu, and Mrs. Dhanalakshmi Koppolu, and my little brother Mouli Krishna Koppolu for their unlimited love and support in all my endeavors. Without their best wishes, I would not have succeeded in my life.

November 18, 2008

ABSTRACT

DEVELOPMENT OF NOVEL MULTILAYERED PARTICLES FOR DRUG DELIVERY AND CELL ISOLATION APPLICATIONS

Bhanu prasanth Koppolu, M.S.

The University of Texas at Arlington, 2008

Supervising Professor: Kytai Truong Nguyen

The objective of this work is to develop multilayered nanoparticles for drug delivery and cell isolation applications. These particles principally consist of three layers; biodegradable polymer, thermo sensitive polymer and magnetic materials. For drug delivery, multilayered nanoparticles (MLNP) consisting of a magnetic core and two encompassing shells made up of temperature sensitive polymer, poly (N-isopropylacrylamide) (PNIPAAm), and biodegradable polymer, poly(D, L lactide-co-glycolide) (PLGA), were developed for targeted and controlled drug delivery. The PNIPAAm layer was immobilized onto magnetic nanoparticles (MNPs) via a silane coupling agent, Vinyltrimethoxysilane (VTMS), and free radical polymerization. These particles were then encapsulated with PLGA using a double emulsion solvent evaporation method with poly (vinyl alcohol) (PVA) as a surfactant. Transmission electron microscopy (TEM) confirmed that multilayered particles were obtained with

PNIPAAm magnetic nanoparticles embedded within the PLGA shell. Factorial design analysis of the results showed that the particles size was inversely proportional to surfactant PVA concentrations and sonication powers while it was directly proportional to PLGA concentrations. PVA concentrations were the most important factor affecting the particle size, while PLGA was the least important factor. The drug release results demonstrated that these multilayer particles produced an initial burst release and a subsequent sustained release of both drugs loaded in the core and shell of MLNP.

For cell isolation, Multi Layered Microparticles (MLMP) with a biodegradable polymeric core and two shells made up of MNPs and PNIPAAm-AH were synthesized. PLGA microspheres loaded with protein were prepared by using a double emulsion method. Magnetic nanoparticles functionalized with silane and silane amide were conjugated onto the surface of the PLGA microspheres by covalently bonding. PNIPAAm-AH copolymer was then immobilized onto the magnetic nanoparticles layer using a coupled silane agent and free radical polymerization of the NIPPAAm and Allylamine (AH) monomers. Scanning electron microscopy (SEM) showed that multilayered particles of size 50 to 100 µm were obtained. The polymeric composition of particles was also confirmed by FTIR spectrum. Differential scanning calorimetric (DSC) analysis determined that the polymer had a lower critical solution temperature (LCST) of 34.9ºC. Conjugation studies showed that the particles could further be conjugated with antibodies. The protein release results demonstrated that these multilayer particles produced an initial burst release and a subsequent sustained release of proteins. The shell release profile was affected by the changes of temperature where

as the core release was affected by the core degradation, shell hydrophilicity, and protein diffusion through the shell. These results show that the particles can be used for impulsive release of differentiating factors followed by slow release of cell enrichment factors. Cell adhesion studies showed that the PNIPAAm-AH surface of the particles supports cell adhesion. Also, cell extraction studies showed that MLMPs can be used to extract cells from a suspension and the isolation process has no significant effect on cell viability.

TABLE OF CONTENTS

LIST OF ILLUSTRATIONS

LIST OF TABLES

LIST OF ABBREVIATIONS

AH – Allylamine

AOT – Docusate sodium salt

APS – Ammonium persulfate

APTMS – 3-Aminopropyltrimethoxysilane

BIS – N,N-Methylenebisacrylamide

BSA – Bovine serum albumin

DCM – Dichloromethane

DLS – Dynamic light scattering

DSC – Differential scanning calorimetry

ECM – Extra cellular matrix

EDC – N-(3-Dimethylamineopropyl)-N'-ethylcarbodiimide hydrochloride

FDA – Federal drug agency

FDS – Flourescien disodium salt

FPS – Flour-PEG-SCM

FTIR – Fourier transform infrared spectroscopy

HCL – Hydrochloric acid

KPS – Potassium persulfate

LCST – Lower critical solution temperature

MLMP – Multilayered microparticles

MLNP – Multilayered nanoparticles

MNP – Mangetic nanoparticles

NHS – N-Hydroxy-succinimide

NIPAAm – N'- isopropylacrylamide

PEG – Polyethylene glycol

PLGA – poly (D, L lactide-co-glcolide)

PNIPAAM – poly (N'- isopropylacrylamide)

PVA – Polyvinyl alcohol

SEM – Scanning electron microscope

SDS – Sodium dodecyl sulfate

SNMNP – Silane amine coated magnetic nanoparticles

TEM – Transmission electron microscope

VTMS - Vinyltrimethoxysilane

CHAPTER 1

INTRODUCTION

1.1 Nanoparticle and Microparticles for targeted drug delivery

Conventional delivery of drugs including oral and intravenous delivery has several disadvantages. One of these draw backs is the inability to target the drug to the site of interest. Another limitation is the inability to control the release of drugs in a therapeutic window for extended periods of time [1]. These limitations emphasize the necessity to develop drug delivery systems which could control the release of drugs over a time course and deliver biologically active compounds selectively to the pathological area [1].

For the past two decades, nano- and micro-particles made of polymers have been investigated for use in targeted and controlled drug delivery. Nanoparticles are solid particles ranging in size from 10nm to 1000nm, whereas microparticles have a size range of 1µm to 1000 µm. These particles consist of various materials, in which biologically active materials (drugs, proteins, and genes) are dissolved, encapsulated, entrapped, adsorbed or attached [2]. The materials to form these particles include natural materials, magnetic materials, non-degradable and biodegradable polymers. Nanoparticles and microparticles can be formulated by a number of different manufacturing methods such as emulsion polymerization, interfacial polymerization, solvent evaporation and solvent deposition [2, 3]. These particulate systems can be tailored to deliver biological active components over a course of time and selectively to the pathological area.

Also, nano/microparticles consisting of contrasting agents can be used to target and effectively visualize biological tissues and cells [4, 5].

1.2 Magnetic nanoparticles

1.2.1 Magnetic nanoparticles as contrasting agents

Magnetic nanoparticles (e.g iron oxide nanoparticles) are currently being used as contrasting agents in the field of Magnetic Resonance Imaging (MRI). These nanoparticles are approved by the Federal Drug Agency (FDA) for clinical use and utilized widely in the 21st century for imaging applications [6, 7]. MNPs are widely used for the diagnosis of inflammatory and degenerative disorders associated with high macrophage phagocytic activity [6, 7]. Magnetic nanoparticles (MNP) are predominantly made of paramagnetic iron oxides like magnetite (Fe_3O_4), maghemite (Fe_2O_3) or other ferrites. The efficacy of the particles as contrast agents is dependent on different factors including the composition, nature of the coating, charge and hydrodynamic size of the coated particles. These factors also determine the particle stability, biodistribution, opsonization, metabolism and clearance from the body [8].

1.2.2 Magnetic nanoparticles as carriers for therapeutic agents

In addition to imaging applications, magnetic nanoparticles are also used to specifically deliver therapeutic agents to certain tissues or cells. The movement and distribution of the MNP can be controlled using an external magnetic field. This property of the MNP can be used to target the particles to the site of interest for therapeutic applications. Also, MNP can be functionalized with chemicals like amino silane, which can be used to conjugate therapeutic agents like drugs

and genes onto MNP [9, 10]. The particle specificity can further be increased by conjugating cell specific targeting ligands onto the surface [11, 12]. This tissue specific MNP are also being investigated for use in hyperthermial cancer therapy.

Hyperthermia is a cancer therapy that consists on heating certain organs or tissues by exposing to external radiation to temperatures between 41ºC and 46ºC causing moderate cellular inactivation or death in a dose-dependent manner. This heating would influence the expression of biomolecules; especially regulatory proteins involved in cell growth and differentiation causing alterations in the cell cycle and subsequently induce cell apoptosis [13]. The classical hyperthermia enhances radiation injury of tumor cells and chemotherapeutic efficacy [14]. Modern clinical hyperthermia trials focus mainly on the optimization of thermal homogeneity at moderate temperatures (42-43ºC) in the target volume, a problem which requires extensive technical manipulations. One way to overcome this problem would be loading tumor cells with targeted magnetic nanoparticles. These nanoparticles would then be heated up using a high frequency external AC magnetic field, causing the death of all particles containing cells [15].

1.2.3 MNP for cell isolation

Isolation and separation of specific molecules by MNP is the most documented and useful application of magnetic particles in various areas of bioscience and nanotechnology. Various magnetic particles have been developed for use in separation processes including purification and immunoassays [12, 13]. Magnetic separation of cells has several advantages in comparison with other isolation techniques. The isolation process permits the target cells to be isolated

directly from crude samples such as blood, bone marrow, and tissue homogenates. Compared to other conventional methods of cell separation, magnetic separation is relatively simple and fast. The static magnetic field does not interfere with the movement of ions and charged solute in aqueous solutions as does the electric field [15]. Furthermore, the large differences between magnetic permeability of the magnetic and non-magnetic materials can be exploited in developing highly specific separation methods [16]. The sheer forces associated with binding and elution is also minimal compared to centrifugation or filtration methods, thereby, increasing the yield of cells. Isolation using MNP also simplifies the procedures like separation and washing which are considered to be tedious steps in conventional cell isolation methods [15]. MNP has been used for isolation of different cells including mammalian, cancerous and stem cells [68-70].

1.3 Polymer encapsulated magnetic nanoparticles

Although magnetic nanoparticles have been used as MRI contrast agents, in hyperthermia treatment for malignant cells and in site specific drug delivery, their application in targeted and controlled drug delivery has been limited. One reason is that magnetic nanoparticles made up of pure iron oxide cannot be loaded with drugs for controlled release [17]. These limitations can be improved by encapsulating MNPs with suitable materials such as polymers, non-polymer materials, and inorganic materials. Encapsulation of MNP also renders them to be more soluble in aqueous or biological media and provides various functional groups on the surfaces for the conjugation of biomolecules.

To produce the polymer MNP, a great variety of polymers have been used. These include natural polymers such as albumin, cellulose, pullulan, and chitosan. Other materials include synthetic polymers like polystyrene, polyethylene glycol (PEG), poly acrylamide, and poly (L-lactic-co-glycolic) acid (PLGA) [19-21]. Furthermore, dextran or liposomes have also been used to coat MNP for drug and gene therapy delivery applications [9, 22, 23]. Of these polymers, temperature sensitive polymers have been generated great interests due to their controlling dug release in response to changes in temperatures.

1.4 Thermo sensitive hydrogels as MNPs coating

1.4.1 Temperature sensitive polymers

Temperature sensitive polymers include poly (N-isopropylacrylamide) (PNIPAAm) and its copolymers [21]. Figure 1.1 shows the chemical structures of NIPAAm monomers (a) and PNIPAAm polymers (b). PNIPAAm undergoes a reversible volume phase transition at a temperature of 32ºC called lower critical solution temperature (LCST). Above the LCST, the hydrogel hydrophobically collapses; expelling water in an entropically favored fashion, whereas the hydrogel retains its hydrophilicity once the temperature goes below LCST and swells in response to the hydrophilic ambience. These reversible swelling and shrinking events have been used as a means to control uptake and release of various therapeutic agents [23-25]. The LCST can also be increased to slightly higher than a body temperature of 37ºC by copolymerizing with a hydrophilic monomer; for example, poly (N-isopropylacrylamide-co-acrylamide) copolymer [24, 25].

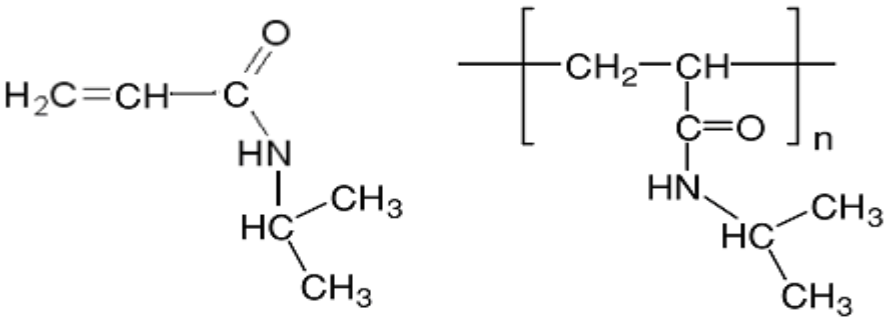

(a) (b)

Figure 1.1: Chemical structure of (a) NIPAAm and (b) PNIPAAm

1.4.2 Thermo sensitive hydrogels for drug delivery and cell culture

Temperature-responsive hydrogels tend to swell or shrink rapidly in response to the external temperature. This volume phase transition of the hydrogels has found various applications, especially in the drug delivery system [28, 29]. For instance, temperature sensitive hydrogels made from NIPAAm and its copolymers act hydrophilic and stay in their swollen state at temperatures below a LCST. As the temperature is increased above the LCST, the hydrogen bonds begin to break and the hydrophobic state becomes more desirable, causing the hdrogels to collapse and shrink, thus releasing the embedded materials. This is a major advantage of these hydrogels. Drugs can be loaded in these hydrogels at low temperatures and then deliver to specific locations where, the drugs will be released when the temperature is increased above the LCST. LCST can be adjusted to required specifications by copolymerization with other monomers. In general, the addition of hydrophilic monomers induces the LCST due to the increase of the hydrogen bonds, which in turn requires higher temperatures for bond breaking. In contrast, the addition of hydrophobic monomers has reverse effects [29].

The thermo-responsive behavior of these polymers can also be used for cell culture. Because cells often attach to the hydrophobic surfaces and detach from the hydrophilic surfaces, thus PNIPAAm have been used to coat surfaces for cell culture and growth. The hydrophobic phase of PNIPAAm acts as an adhesive surface for cells and the hydrophilic phase act as a releasing surface [30, 31]. As the temperature drops below 32^{o}C, the PNIPAAm chains rapidly hydrate causing the cells to detach from the surface [32]. This behavior is advantageous because it eliminates the need for enzymatic or mechanical detachment of cells allowing them to retain their morphology and function as shown in Figure 1.2. It has been found that enzymatic and mechanical detachment can disrupt the cell membrane and cause a change in cellular activities [33].

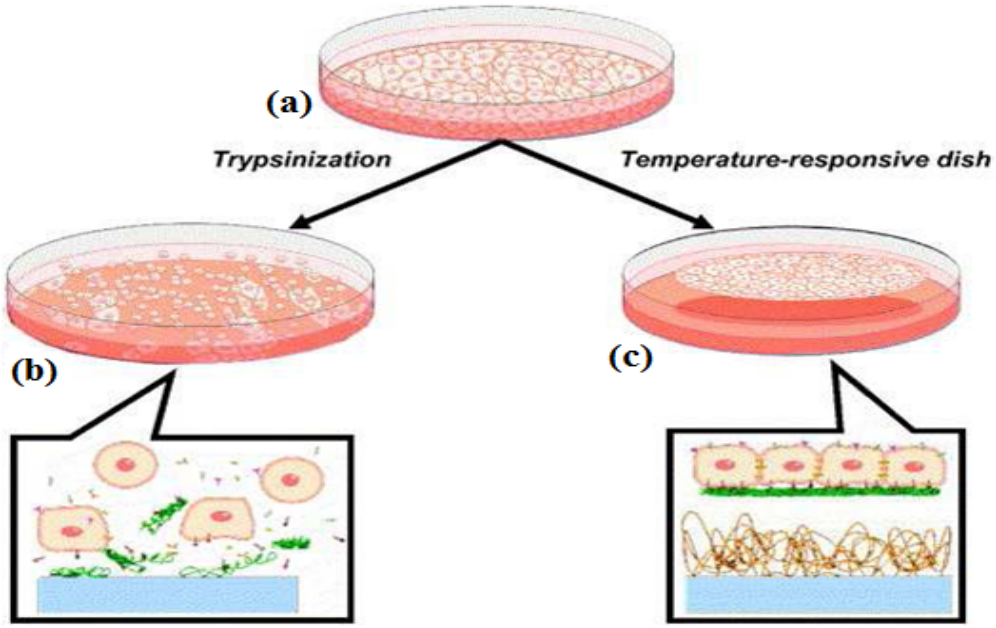

Figure 1.2: Temperature-responsive culture dishes [33]. (a) During culture, cells deposit extracellular matrix (ECM) molecules and form cell-to-cell junctions. (b) With typical proteolytic harvest by trypsinization, both ECM and cell-to-cell junction proteins are degraded for cell recovery. (c) Cells harvested from temperature-responsive dishes are recovered as intact sheet along with deposited ECM

1.5 Objective of the research project

As described above MNPs either coated with biodegradable polymers or thermosensitive polymers have lots of advantages for use in drug delivery and tissue engineering applications. The aim of our project is to develop novel multilayered particles for drug delivery and cell isolation. This particles posses all magnetic, degradable and thermosensitive components and can be loaded with two drugs/proteins. Also, these particles can be conjugated with targeting ligands/antibodies which facilitates for specific drug delivery and cell isolation. The research aims and advantages of developed multilayered particles specifically for drug delivery and cell isolation will be discussed in detailed in the upcoming chapters.

Specific aims of our project are

Aim 1. Develop multilayered magnetic nanoparticles for drug delivery

Aim 2. Develop multilayered magnetic microparticles for cell isolation

CHAPTER 2

DEVELOPMENT OF MULTILAYERED NANOPARTICLES FOR DRUG DELIVERY

2.1 Introduction

Although magnetic nanoparticles have been used as MRI contrast agents, in hyperthermic treatment for malignant cells and in site specific drug delivery [6-8, 13, 14], their application in targeted and controlled drug delivery has been limited. One reason for this is that magnetic nanoparticles made up of pure iron oxide cannot be loaded with drugs for controlled release [34]. Thus the incorporation of magnetic nanoparticles with polymers such as PLGA has been used to increases their biocompatibility and ability for controlled drug delivery via the degradation of PLGA polymer [32, 33]. In addition, thermo sensitive poly(N-isopropylacrylamide) (PNIPAAm) copolymer based nanoparticles with magnetic cores have been developed to provide a temperature sensitive drug release mechanism [35, 36]. These nanoparticles can be loaded with a hydrophilic drug and guided to the treatment site by an external magnetic field. Then, an external electromagnetic device can be used to locally raise the temperature above the polymer's Lower Critical Solution Temperature (LCST); consequently, the polymer structure collapses and releases the drug. Polymer coated magnetic particles often consist of core-shell based nanostructures. The magnetic core allows a magnetic based targeting mechanism and serves as an MRI contrast agent, whereas the shell is used to enhance the particle biocompatibility while allowing drug loading and release.

The objective of our research is to develop dynamic nanoparticles capable of providing a dual drug delivery mechanism. To reach our goal, Multi Layered Nanoparticles (MLNPs) with a magnetic core and two shells made up of PNIPAAm and PLGA, as shown in Figure 2.1, were synthesized. PNIPAAm was immobilized onto the magnetic nanoparticles using a coupled silane agent and free radical polymerization of the N-isopropylacrylamide (NIPPAAm) monomer. The resultant PNIPAAm magnetic nanoparticles were encapsulated with PLGA by a double emulsion solvent evaporation technique [37-39]. The morphology, size and size distribution of these multilayered nanoparticles were determined by transmission electron microscope (TEM) and Dynamic Light Scattering (DLS) technology. The effect of different factors including surfactant PVA concentration, PLGA concentration and sonication power on the particle size were determined using factorial analysis. The iron particle concentration, drug loading and release from the selected particles of 300nm (the smallest particles obtained from factorial analysis) were also studied.

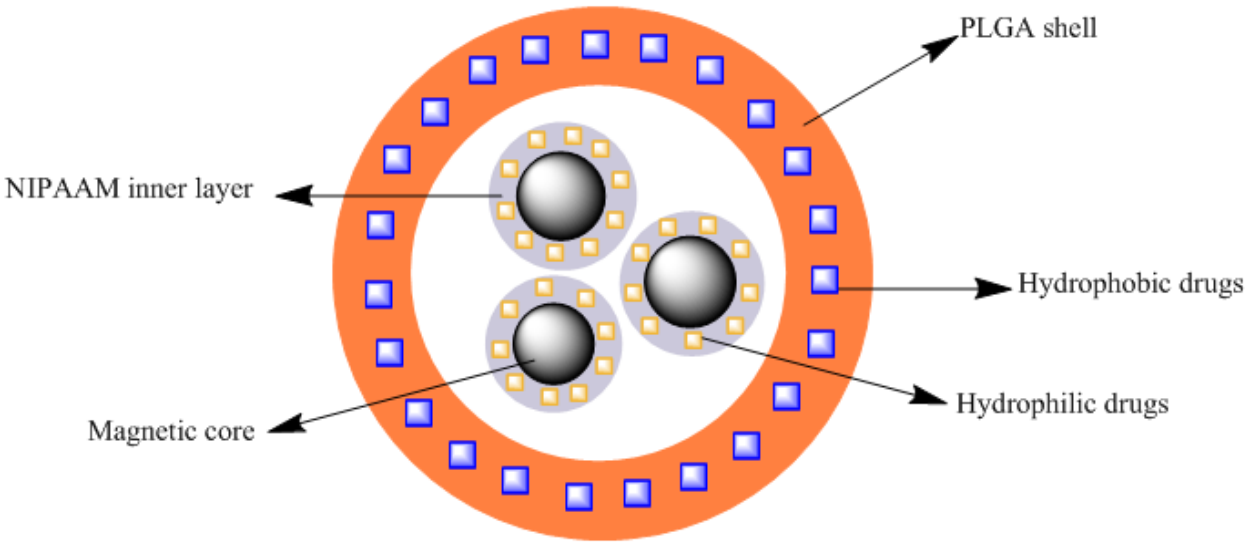

Figure 2.1: Magnetic PNIPAAm PLGA core shell multilayered particle design

2.2 Materials and Methods

2.2.1 Materials

Poly (D, L lactide-co-glycolide) (PLGA, 50/50, Birmingham Polymers), N-Isopropylacrylamide (NIPAAm, 97% Aldrich), Docusate sodium salt (AOT, Sigma-Aldrich), Sodium dodecyl sulfate (SDS, 99%, Sigma-Aldrich), N,N-Methylenebisacrylamide (BIS, Sigma), Potassium persulfate (KPS, 99+%, Sigma-Aldrich), Dichloromethane (DCM, MERCK KGaA), Vinyltrimethoxysilane (VTMS, 98%, Aldrich) and Poly(vinyl alcohol) (PVA, 87-89%, Sigma-Aldrich) were used as obtained.

2.2.2 Preparation of magnetic nanoparticles

Magnetic nanoparticles were synthesized in our lab using a co-precipitation method of ferrous and ferric salts in the presence of a basic solution and the surfactant AOT [34, 35]. In brief, Ferric chloride hexahydrate and Ferrous chloride tetrahydrate (2:1) were dissolved in 600 ml of De-ionized (DI) water. After purging the solution with argon gas, 0.36g of AOT in 16 ml of hexane was added and the solution was heated to 85°C. At this temperature, NaOH (7.1 M) was added. After a 2-hour reaction period, particles were washed extensively with ethanol and then centrifuged at 25000 rpm for 45 minutes. The magnetic nanoparticles were dried in a vacuum oven.

2.2.3 Preparation of VTMS–coated magnetic nanoparticles

The magnetic nanoparticles were coated with VTMS via acid catalyst hydrolysis, followed by electrophilic substitution of ferrous oxide on the surface of the magnetic nanoparticles [35, 36]. In brief, 0.48ml of VTMS was hydrolyzed using 3% acetic acid in the presence of 99% ethanol in water. 0.074g of magnetic nanoparticles were then dispersed by sonication at 100 W for 30 minutes in this solution; the VTMS coated magnetic nanoparticles were then obtained after 24 hours of vigorous mechanical stirring at room temperature. The product was excessively washed with a mixture of water/ethanol (1:99 v/v) to remove un-reacted components. The VTMS-coated magnetic particles were collected using a magnet and dispersed in water before the next step**.**

2.2.4 Immobilization of PNIPAAm on the surface of magnetic nanoparticles

VTMS–coated magnetic nanoparticles were used as a template to polymerize NIPAAm as previously described [45]. In brief; 0.028g of VTMS-coated magnetic nanoparticles, 0.15g of NIPA, 0.0131g of BIS (a cross-linking agent), and 0.041 g of SDS (a surfactant) were sonicated in cold water for 30 minutes. Then, the mixture was heated to 70°C and a 0.078g of KPS was added to initiate the reaction. The solution was stirred under Argon for four hours. The product was purified several times with DI water using a magnet to isolate and collect PNIPAAm-coated magnetic nanoparticles.

2.2.5 Encapsulation of PNIPAAm magnetic nanoparticles with PLGA

PNIPAAm magnetic nanoparticles were encapsulated with PLGA using a double emulsion solvent evaporation method similar to that used to encapsulate bare iron oxide [46] or magnetic nanoparticles [47]. Initially, 15mg of PNIPAAm magnetic nanoparticles were dispersed in 300µl DI water, and this particle dispersion was added to 3% w/v PLGA in 3ml of DCM. The solution was then sonicated for 30 seconds at 55W using a Micronix 3000 sonicator to obtain the primary w/o emulsion. The emulsion solution was added drop wise into a 2% w/v PVA solution, and the mixture was then sonicated for 2 minutes at 55W power to obtain a w/o/w emulsion. After stirring overnight to allow solvent evaporation, our multi-layer magnetic nanoparticles were collected using a magnet, washed several times with DI water to remove bare PLGA particles, and then centrifuged at 15000 rpm for 20min (Beckman LM100 ultracentrifuge) to remove residual PVA.

2.2.6 Size and morphological characterization of the multi-layer nanoparticles (MLNPs)

The obtained MLNPs were characterized for size and morphology using Transmission Electron Microscope (TEM) imaging and light dispersion methods, respectively. For TEM, nanoparticles were placed on a plasma activated grid and observed using TEM (1200, JEOL) to determine the size and morphology of the particles. The size and size distribution of the nanoparticles were also determined by a Dynamic Light Scattering method (Nanotrac^{TM}, Microtrac 150).

2.2.7 Effects of different factors on particle size

The factorial studies were conducted to evaluate the effects of different factors on the size of particles. Statistical analysis software Design Expert™ (Version 11, Statease™) was used for the analysis. A half-factorial experiment (4 runs instead of 8) for three factors was designed. The three factors (independent variables) included PVA concentration (2% and 5% w/v), PLGA concentration (2% and 3% w/v), and sonication power (35 and 55W). The evaluated response (dependent outcome) was the particle size. The resulting factorial design is shown in Tables 2.1 and 2.2. To evaluate the effects of factors on particle size, particles were synthesized for each run and their sizes were analyzed using TEM and DLS. After the analysis, particles of 300nm size obtained for 3rd run were used for later studies.

Table 2.1: Variables used for half factorial experimental design

Factors	**High**	**Low**
PVA concentration	60mg (5% w/v)	24mg (2% w/v)
PLGA concentration	90mg (3%w/v)	60mg (2% w/v)
Sonication power	55W	35W

Table 2.2: Half factorial experimental variables used for preparation of PLGA coated PNIPAAm magnetic core shell nanoparticles

Exp. No.	**PVA conc.**	**PLGA conc.**	**Sonication power**
1	2%	3%	35W
2	5%	2%	35W
3	5%	3%	55W
4	2%	2%	55W

2.2.8 Determination of iron oxide concentration

Iron oxide concentration was determined by digesting the particles with HCL and applying the spectrophotometric method on these samples [48]. In brief, 2mg of MLNPs were suspended in 1ml DI water and 1ml of 30% v/v HCL was added to the particles. The solution was incubated at 40°C for 2 hours to initiate breakdown. 1ml of 1% w/v Ammonium persulphate was added to oxidize the ferrous ions present in the above solution to ferric ions. In all, 1.0 ml of Potassium thiocyanate (0.1M) was added to this solution and shaken for 15min to form the Iron-thiocyante. After incubation, the absorption of this solution was read at a wavelength of 540nm and compared with standards to get the amount of iron oxide presented in the particles.

2.2.9 Drug loading and release studies

Bovine serum albumin (BSA) and curcumin were used as hydrophilic and hydrophobic model drugs. BSA (20mg) was first loaded into PNIPAAm magnetic nanoparticles (60 mg) that were suspended in 20ml DI water. The solution was left on a shaker for 3 days at 4ºC to let the drug absorb into the particles. These loaded PNIPAAm magnetic nanoparticles were used to form the multilayer nanoparticles as described earlier. Second, curcumin was loaded by mixing 9mg of curcumin along with 90mg of PLGA in 3ml of DCM during the emulsion method described above. Thus, curcumin was embedded in the PLGA layer while BSA was loaded into the inner PNIPAAm layer.

Loading efficiency was calculated indirectly. Here, the amount of drug left in the supernatant after removing the drug-loaded particles was determined. This amount was subtracted from the initial concentration of drug to get the percentage of loading efficiency (Equation 1).

$$\text{Percentage loading efficiency} = \frac{(\text{Original conc} - \text{Supernatant conc})}{\text{Original conc}} \times 100 \qquad (1)$$

To study the amount of drug released at a certain time, the drug loaded particles were suspended in a known amount of PBS. Samples are dialyzed at 4ºC and 37ºC respectively, and the dialysate was collected and replaced by fresh PBS at regular intervals of time up to a maximum of 3 weeks. The collected samples were stored at -20ºC until analysis. The samples were analyzed for BSA release amount using BCA^{TM} protein assays (Pierce) following the manufacturer's instructions. To determine the released curcumin, the supernatant samples were mixed with ethanol at a 1:1 ratio to completely ensure the curcumin solubility. The absorbance of samples

was read at 490nm, and the curcumin solutions with various concentrations were used to obtain a standard curve. The amount of BSA released at 4ºC and 37ºC and for curcumin at 37ºC was plotted versus time to get the drug release profile of the particles.

2.3. Results and Discussion

2.3.1 Size and morphological characterization of the particles

As shown in Figure 2.2, our multilayer particles obtained from initial PVA, PLGA concentrations of 1% w/v, 3% w/v respectively, and sonication power of 35W are in the range of 500-1000nm using TEM. The MLNPs have a solid spherical morphology with a non-uniform rough surface, due to the presence of PNIPAAm magnetic nanoparticles on the PLGA shell. It is evident from the images that the PNIPAAm magnetic nanoparticles are present in the core as well as the outside of the microparticles. The attachment of the PNIPAAm magnetic nanoparticles onto the outer surface can be attributed to the surface charge interaction between the polymers and the magnetic attraction between the particles.

2.3.2 Effect of PVA, PLGA concentration and sonication power on the multilayer nanoparticle size

The size of the particles depends on the droplet size formed during the emulsion step and can be easily reduced by varying the factors like sonication power and surfactant concentration [47]. Thus, these factors were selected to study their effects on the synthesized particle size in our

study. The average size of the particles measured using TEM was compared with DLS (Figure 2.3). A half normal probability plot was obtained using the Designexpert^{TM} software to

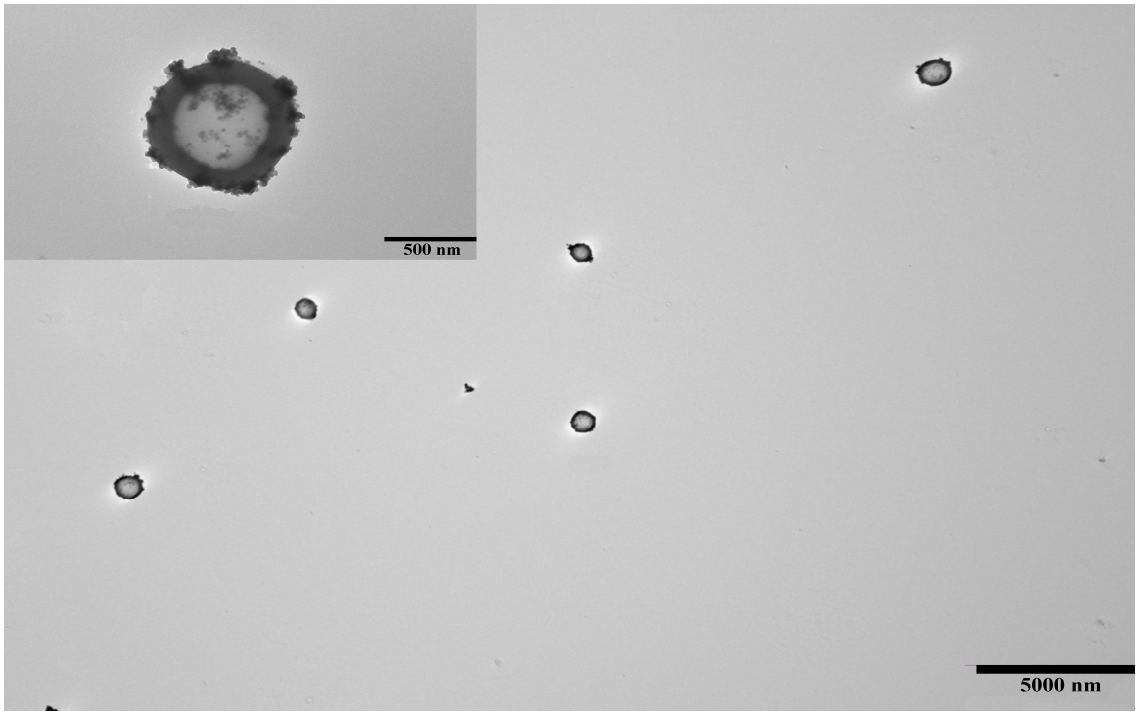

Figure 2.2: Transmission electron microscopic image of multilayered particles

demonstrate the relative importance of these factors. The absolute values of effects are represented on the X-axis as squares and estimates of errors are represented as triangles (Figure 2.4a). The effects towards the right side of the plot are real effects, and the farther the factors are from the zero region, the more significant the effects are. The most important factors that affected the particle size were sonication power and PVA concentration. These two factors have a negative effect on the particle size. This means that increasing the sonication power and PVA concentration would decrease the particle size. On the other hand, PLGA concentration is

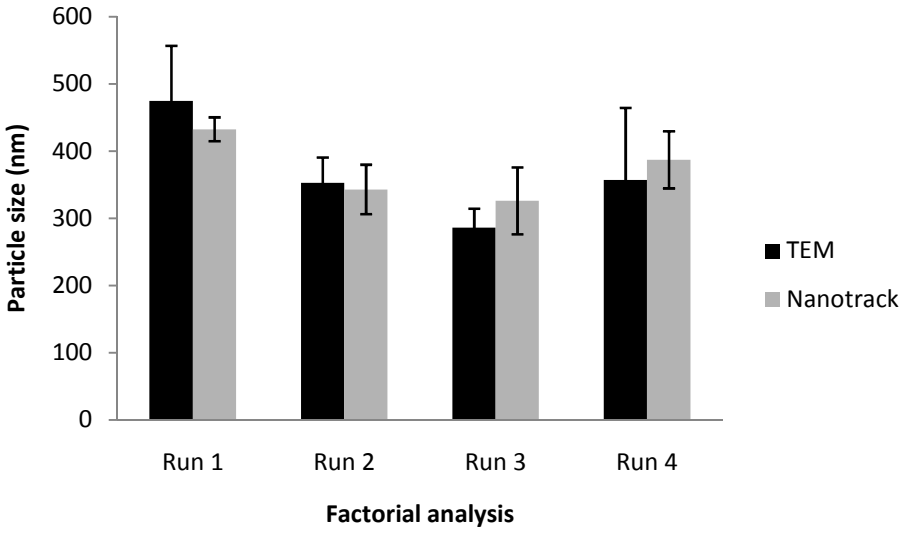

Figure 2.3: Size of the particles obtained by factorial design.

the least important factor and has a positive effect on particle size. The response surface diagrams were developed using Design Expert™ to study the relationship between the factors and particle size. Figure 2.4(b) shows that, at a PLGA concentration of 2.5% w/v, it is evident that increasing the sonication power (from 35W to 55W) and the PVA concentration (from 2% to 5% w/v) has the largest effect on reducing particle size. At a PVA concentration of 3.5% w/v (Figure 2.5a) and a sonication power of 45W (Figure 4d), the particle size increased slightly with an increase in PLGA concentration (from 2% to 3% w/v), though not significant. In comparison with PLGA concentration, sonication power (Figure 2.5a) and PVA concentration (Figure 2.5b) changed particle size significantly. These observations are consistent with other studies which show that the size of the particles prepared by emulsion methods can be effectively controlled by varying surfactant concentration and sonication speed [49-51]. These results suggest that the size of the formed emulsion droplets depends mainly on the surfactant concentration and homogenization speed/power in emulsion methods.

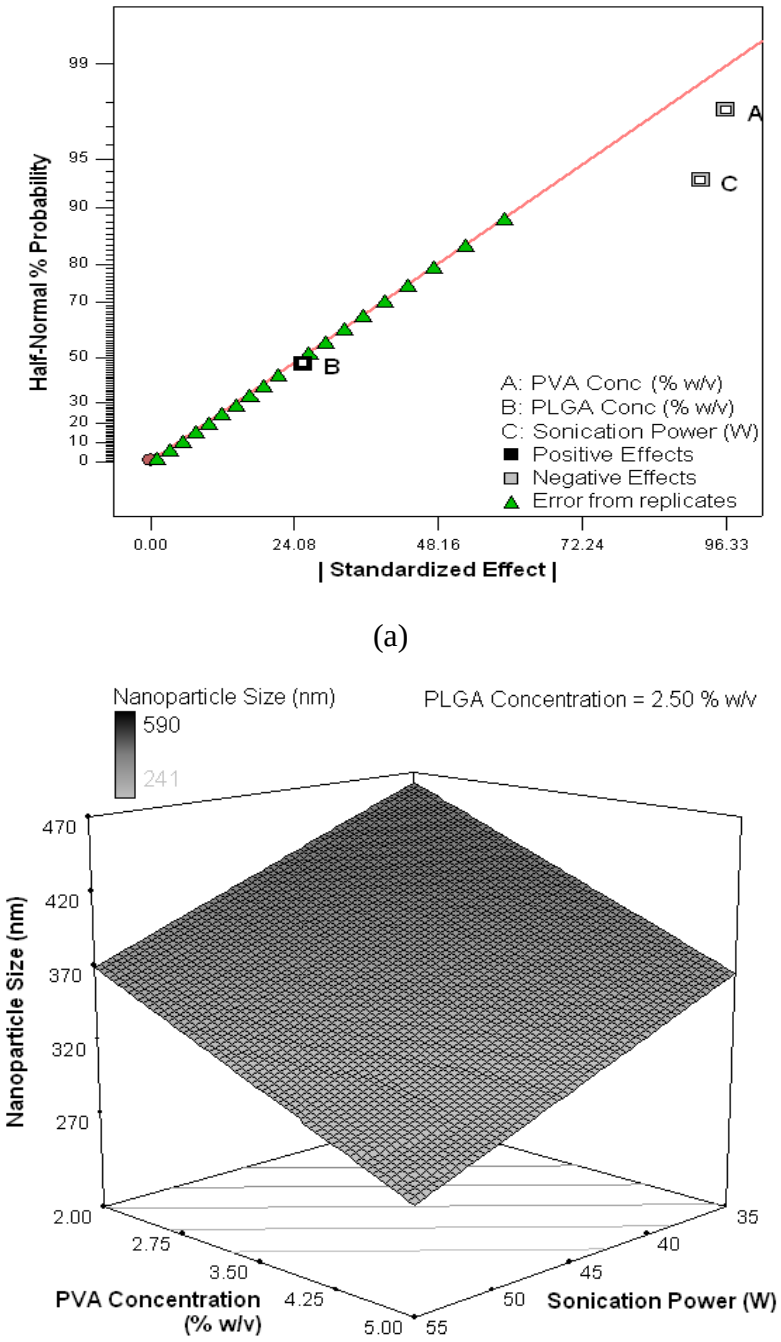

Figure 2.4: a) Half-normal plot showing the effect of factors on the particle size, b) Surface plot showing the effect of PLGA concentration

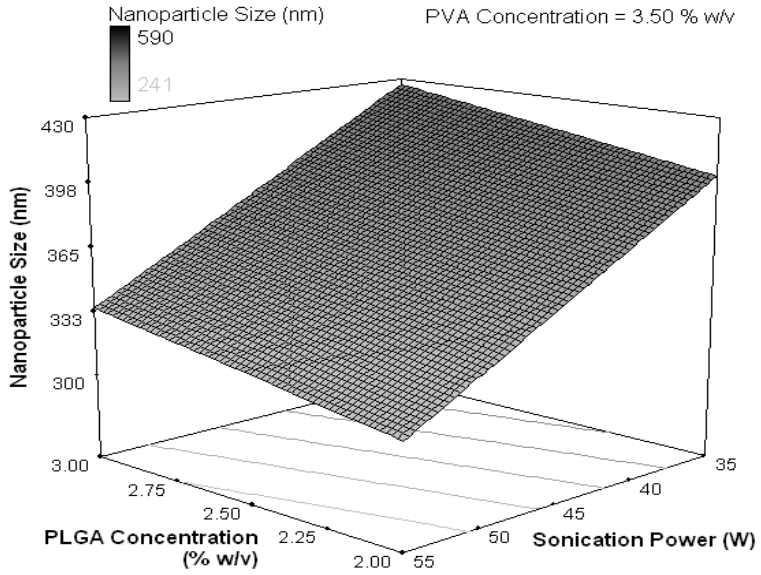

(a)

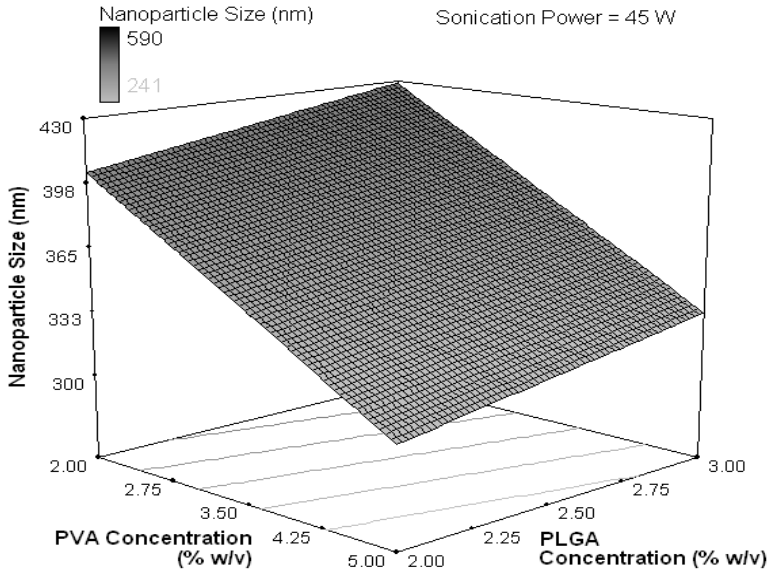

(b)

Figure 2.5: Surface plot showing the effect of a) PVA concentration, b) sonicaton power on the particle size

The equation for nanoparticle size in terms of actual factors was obtained from factorial analysis. The predicted nanoparticle size can be calculated for any combination of individual factors within the range provided in Table 2.1 using the following equation:

Particle size (nm) = 624.71 – 32.17 × (PVA conc) + 25.50 × (PLGA conc) – 4.63 × (Sonication Power)

2.3.3 Iron oxide concentration of multilayered nanoparticles

The iron oxide concentration of the samples (n=4) from Run 3 was measured to quantify the magnetic particles to polymer ratio of the resultant MLNPs. Weight/weight of the iron oxide concentration in the multilayered particle varied from 70 to 75%, with the remaining 25 to 30% being made of PNIPAAm and PLGA. These results confirm that magnetic particles are successfully encapsulated by PNIPAAm and PLGA. The high iron oxide content is due to the higher density of iron oxide compared to the polymer and the presence of non-encapsulated magnetic nanoparticles, which cannot be eliminated. Bare polymeric particles are eliminated by the magnetic extraction process during synthesis.

2.3.4 Drug release profile of the multilayered nanoparticles

BSA and curcumin were selected as hydrophilic and hydrophobic model drugs because they can easily be quantified. BSA was loaded into the PNIPAAm layer, whereas curcumin was incorporated in the biodegradable PLGA shell. The loading efficiency of curcumin into PLGA

was approximately 49.5%, which is consistent with other studies [51, 52] where hydrophobic drugs were incorporated into PLGA particles using an emulsion method. The loading efficiency of BSA into the PNIPAAm layer was approximately 65% which is lesser than that obtained in other studies [35, 36] where the hydrophilic drug was incorporated into PNIPAAm based magnetic nanoparticles. This indicated that some BSA was released from the PNIPAAm magnetic nanoparticles during encapsulation with PLGA.

The release characteristics of curcumin from our nanoparticles showed a burst effect within one day, followed by a sustained release for the remaining 13 days with approximately 35% of the total encapsulated drug being released. As shown in Figure 2.6(a) about 14% of the total drug (curcumin) encapsulated was released within 12 hours due to a burst effect. This might be due to the drug being adsorbed onto the particle. This result is consistent with other studies of drug loaded PLGA particles [52]. As shown in Figure 2.6(b), the percent of cumulative release of BSA at 37ºC was significantly higher than at 25ºC. This is consistent with previous studies [35, 36] where drug released from the PNIPAAm magnetic nanoparticles was studied and is indicative of the temperature sensitive drug release from the PNIPAAm layer. After 2 weeks, 53% of the encapsulated BSA was released at 25ºC, whereas at 25ºC approximately 34% was released. About 28% of BSA was released due to the initial burst effect followed by a sustained release after 12 hours contrary to previous studies on PNIPAAm based drug delivery systems where even a higher amount of drug was released due to burst a effect which lasted for longer periods of time [36]. The low BSA release might be due to the inability of BSA released from the PNIPAAm layer to pass through the outer PLGA layer. Thus, the release of both model drugs might be dependent on the degradation of PLGA. Also, an initial burst BSA release can be

partly attributed to the release from the PNIPAAm magnetic particles attached to the surface of the PLGA shell.

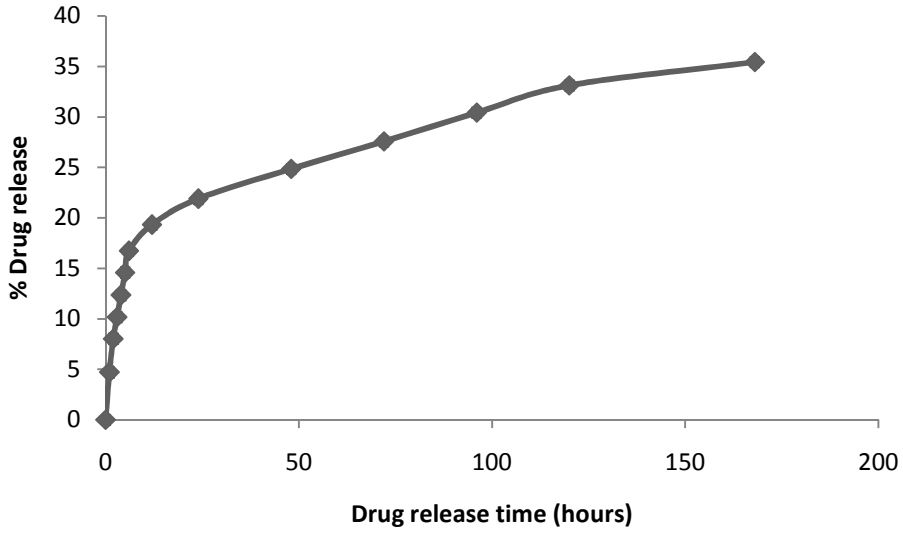

(a)

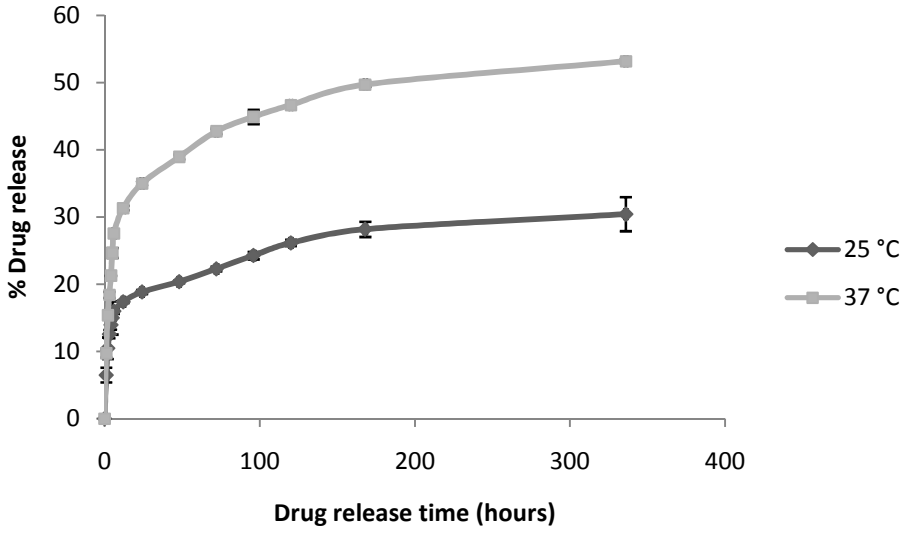

(b)

Figure 2.6: Drug release studies (a) Curcumin release, (b) BSA release

2.4 Conclusion

In this study we have systematically developed a novel multilayered particle that consists of a PNIPAAM magnetic core and PLGA shell which can be loaded with two drugs, one hydrophilic and the other hydrophobic. Our study shows that the particle size can be controlled by varying the PVA concentration and sonication power. We were able to successfully load the particles with BSA and curcumin, models for hydrophilic and hydrophobic drugs. Particles provided a sustained release of curcumin throughout the two weeks of study, whereas the BSA release was characterized by an initial burst release followed by a sustained release. The BSA release at 37°C was also significantly more than that at 25°C suggesting a temperature responsive drug release.

Though we were successful in developing multilayered particles which can be loaded with two drugs by encapsulating PNIPAAm magnetic nanoparticles with PLGA, the applicability of the particles for drug delivery may have some limitations. As seen in the TEM images, not all of the PNIPAAm magnetic nanoparticles were encapsulated and few were present on the surface of the nanoparticles. This would affect the particle size and hinder the drug release mechanism as observed during the drug release studies. Also, the presence of the PNIPAAm magnetic particles on the surface reduces the number of carboxylic groups available for future conjugation with the targeting moieties. Another limitation is that a few of the PNIPAAm magnetic nanoparticles were encapsulated in the PLGA shell instead of a single particle encapsulation. This would affect the particle size. In the future we will try to minimize the un-encapsulated PNIPAAm magnetic particles by careful adjustment of the parameters, and we will investigate methods to improve our MLNPs.

CHAPTER 3

DEVELOPMENT OF MULTILAYERED MICROPARTICLES FOR CELL ISOLATION

3.1 Introduction

Magnetic nanoparticles are currently being used for several cell isolation applications including immunogenic magnetic separation [53, 54] and microbial cell separation [55,56]. Cell separation with magnetic colloidal labels [57] and isolation of cells that specifically express surface carbohydrate binding molecules using carbohydrate (e.g. cellulose, sucrose etc) coated magnetic beads [58] have also been studied. In all cell isolation applications, MNPs are used to target and isolate a particular cell type using a ligand-receptor based mechanism. However, conventional magnetic nanoparticles do not support cell adhesion onto their surface and thereby subsequently cell growth. Another problem with the conventional MNP based cell isolation systems is that they cannot be loaded with proteins, growth factors that can be used for enrichment or stem cell differentiation. These limitations of the MNP can be resolved by coating the MNP with a polymeric layer that can be loaded with biological active components like growth factors and release them in a controlled release rate.

The objective of our research is to develop a multi layered core shell microparticles that can be used for magnetic cell separation, enrichment and stem cell differentiation. The advantage of these microparticles is that they can be used to isolate cells without any use of chemicals like Ficoll or shear force involved in conventional cell isolation procedures which are harmful to

sensitive cells like stem cells. Also, these MLMPs can be loaded with proteins that can be used for cell enrichment or even stem cell differentiation. To reach our goal, Multi Layered Microparticles (MLMPs) with a biodegradable polymeric core and two shells made up of MNPs and PNIPAAm as shown in Figure 3.1 were synthesized. PLGA microspheres loaded with biological active components were prepared using a double emulsion method [60]. Magnetic nanoparticles were incorporated onto the surface of the PLGA microspheres by covalently bonding of silane amide of functionalized MNP with the carboxylic acid (COOH) groups presented on PLGA surface in the presence of carbodiimide [61]. PNIPAAm-AH copolymer was then immobilized onto the magnetic nanoparticle layer using a coupled silane agent and free radical polymerization of the N-isopropylacrylamide (NIPPAAm) and Allylamine (AH) monomers [35, 36]. The morphology, size and size distribution of these multilayered particles were determined by Scanning Electron Microscope (SEM). The chemical composition of the microparticle was investigated utilizing Fourier Transform Infrared Spectroscopy (FTIR). LCST was determined by visual observation and differential scanning calorimetry (DSC). The conjugation capability of the synthesized microparticles was assessed by incorporating fluorescent PEG and antibodies onto nanoparticles, and their fluorescence was imaged via an enhanced optical microscope (Cytoviva). The protein release behaviors of the microparticle biodegradable core alone at temperatures of 37ºC and shell alone at temperatures of 25ºC and 37ºC were analyzed using bovine serum albumin (BSA) as a protein model. Also, simultaneous protein release behavior of both the core and shell of the microparticle at temperatures of 25ºC and 37ºC were analyzed by using BSA as a hydrophilic model for the core release and fluorescein disodium salt (FDS) as a hydrophilic model for the shell release.

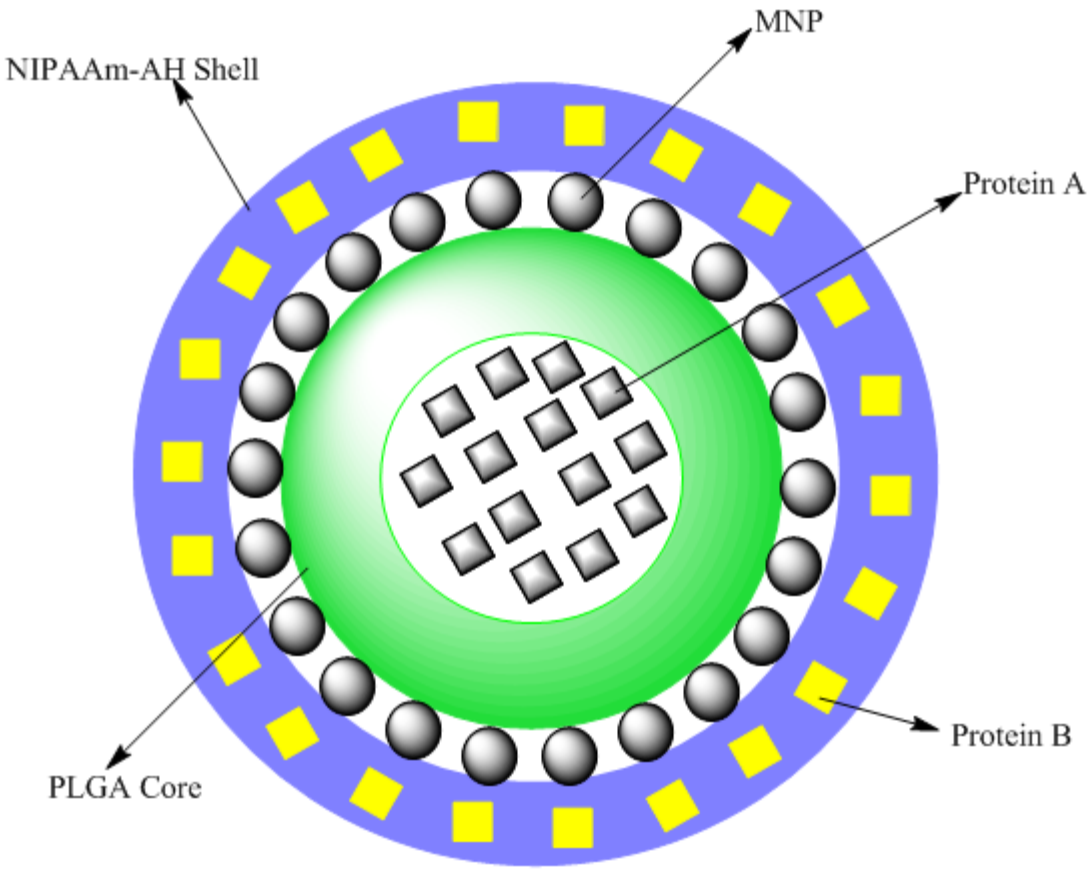

Figure 3.1: Design of Multilayered core shell microparticles

3.2 Materials and methods

3.2.1 Materials

Poly (D, L lactide-co-glycolide) (PLGA, 50/50, Birmingham Polymers), N-Isopropylacrylamide (NIPAAm, 97% Aldrich), Allylamine (AH, 99% Aldrich), Docusate sodium salt (AOT, Sigma-Aldrich), Sodium dodecyl sulfate (SDS, 99%, Sigma-Aldrich), N,N-Methylenebisacrylamide (MBA, Sigma), Ammonium persulfate (APS, 99+%, Sigma-Aldrich), Dichloromethane (DCM, MERCK KGaA), Vinyltrimethoxysilane (VTMS, 98%, Aldrich), 3-Aminopropyl-trimethoxysilane (APTMS, 95%, Acros organics) Flourescein disodium salt (FDS, Acros organics), Bovine serum albumin (BSA, Sigma), N-(3-Dimethylamineopropyl)-N'-ethylcarbodiimide hydrochloride (EDC, SIGMA), N-Hdroxy-succinimide (NHS, 98%, Aldrich) and Poly(vinyl alcohol) (PVA, 87-89%, Sigma-Aldrich) were used as obtained. Cell culture media and supplements were obtained from Invitrogen, whereas serum was purchased from HyClone

3.2.2 Preparation of PLGA micro particles

PLGA microparticles loaded with BSA were prepared using a double emulsion solvent evaporation method [62-65]. In brief, 100mg of PLGA was dissolved in 5ml DCM (10% w/v) to form the organic phase. BSA solution (20mg of BSA dissolved in 200µl deionized water) was added to the organic phase and sonicated for 30sec at 50W power using a sonicator (Biologics, Inc. 330 V/T) to form a primary emulsion. The resultant solution was then emulsified with 20 ml of 0.5% w/v PVA solution at a speed of 450 rpm using magnetic stirrer to produce a

secondary emulsion. The solution was then left on the magnetic stirrer overnight to allow solvent evaporation, and the microparticles were isolated by centrifugation, washed 5 times in DI water and freeze dried.

3.2.3 Preparation of magnetic nanoparticles

Magnetic nanoparticles were synthesized in our lab using a co-precipitation method of ferrous and ferric salts in the presence of a basic solution and the surfactant AOT [35, 68]. In brief, Ferric chloride hexahydrate and Ferrous chloride tetrahydrate (2:1) were dissolved in 600 ml of De-ionized (DI) water. After purging the solution with argon gas, 0.36g of AOT in 16 ml of hexane was added and the solution was heated to 85°C. At this temperature, NaOH (7.1 M) was added. After a 2-hour reaction period, particles were washed extensively with ethanol and then centrifuged at 25,000 rpm for 45 minutes. The magnetic nanoparticles were dried in a vacuum oven.

3.2.4 Functionalization of MNPs with silane and silane amine

The magnetic nanoparticles were coated with VTMS and APTMS via acid catalyst hydrolysis, followed by electrophilic substitution of ferrous oxide on the surface of the magnetic nanoparticles as shown in Figure 3.2 (a) [35, 66-68]. In brief, 0.23ml of VTMS and 0.28ml of APTMS was hydrolyzed using 3% acetic acid in the presence of 99% ethanol in water. 0.074g of magnetic nanoparticles was then dispersed by sonication at 100 W for 30 minutes in this solution. Silane and amine coated magnetic nanoparticles (SNMNPs) were then obtained after

24 hours of vigorous mechanical stirring at room temperature. The product was excessively washed with a mixture of water/ethanol (1:99 v/v) to remove un-reacted components. The surface functionalized magnetic particles were collected using a magnet and were dispersed in water before the next step**.**

3.2.5 Coating functionalized MNPs onto the PLGA microparticle surface

Surface functionalized MNPs were coated onto the PLGA microparticles using carbodiimide chemistry [69]. In brief, 20mg of PLGA microparticles were dispersed in 90ml 0.1% w/v MES buffer under stirring. 14mg of SNMNPs and 5mg SDS were added to 10ml MES buffer and were dispersed by sonication at 50W power. The SNMNPs solution is then added to the PLGA particle solution along with 0.16g of EDC and 0.16g of NHS, respectively. The solution was left on the magnetic stirrer for 6 hours to allow the reaction. The SNMNPs coated PLGA microparticles were then isolated by centrifugation, washed 5 times in DI water and freeze dried.

3.2.6 Immobilization of PNIPAAm-AH on the surface of SNMNPs coated PLGA microparticles

PLGA-MNPs microparticles were used as a template to polymerize NIPAAm and AH in an aqueous micelle solution as shown in Figure 3.3. SDS and BIS were used as surfactant and cross linking reagents, respectively, as previously described [35, 66]. In brief, 0.008 g of PLGA-MNPs, 0.1 g of NIPAAm, 0.1 ml of AH, 0.0035 g of BIS, and 0.0005 g of SDS were sonicated at 20W in 3ml cold water for 2 minutes. 0.0096 g of APS and 1.3 µL of TEMED were added to the solution. The reaction was carried out at room temperature under Argon for 4 hours with

vigorous mechanical stirring. The product was purified several times with DI water by centrifugation at 500 RPM for 5 min to collect our MLMPs, and these particles were freeze-dried before use.

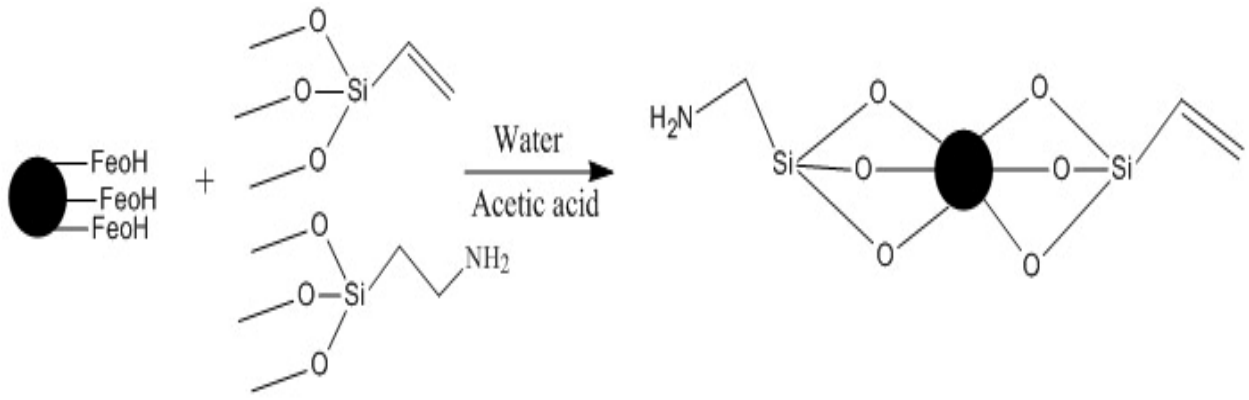

(a)

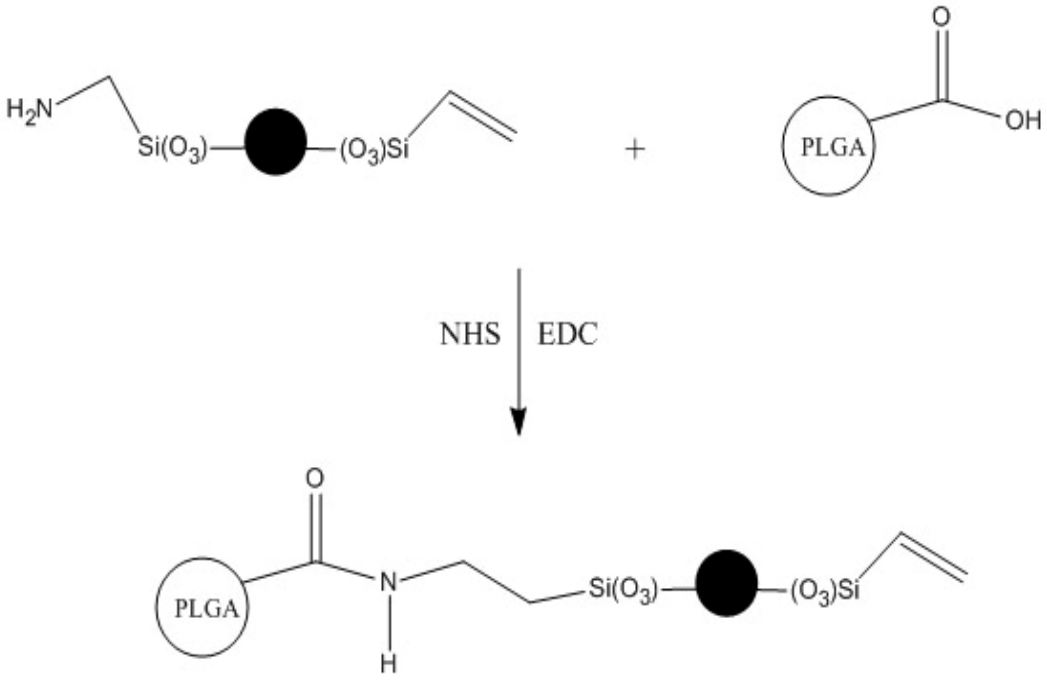

(b)

Figure 3.2: Preparation procedure of (a) Coating MNP with VTMS and APTMS (b) Coating SNMNPs onto the PLGA microparticles

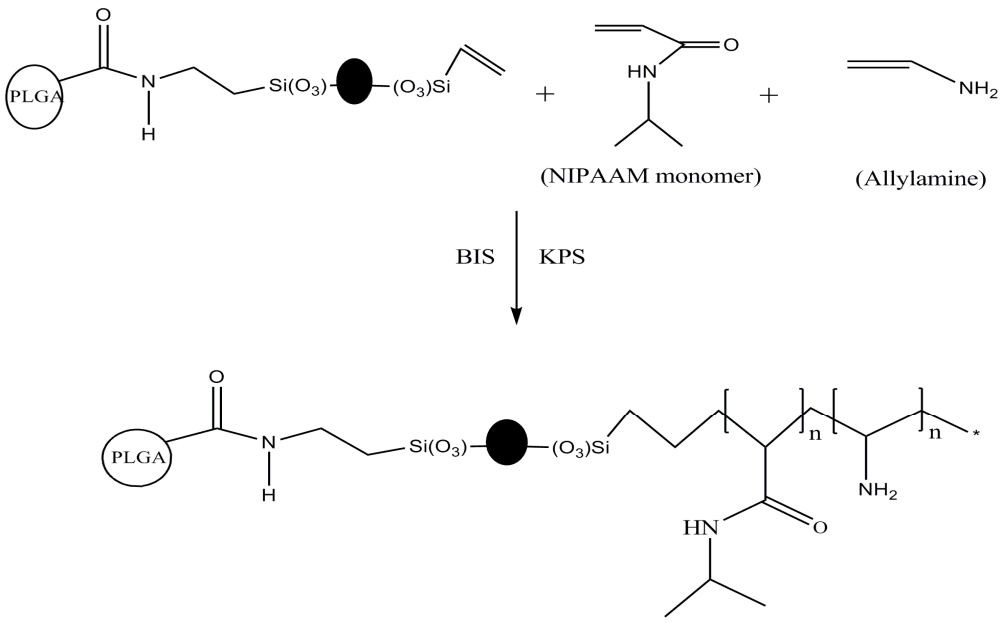

Figure 3.3: Immobilization of NIPAAm – AH on magnetic layer

3.2.7 Size and morphological characterization of the multi-layer microparticles (MLMPs)

Scanning electron microscopy (SEM, Hitachi N3000) was used to determine the size and shape of the synthesized microparticle. In general, samples were prepared by drop casting the microparticle dispersed water solution onto a glass slide. The samples are then air dried and surface coated with silver (Ag) using sputter coating system (Thermo electron, Nicolet 6700) before observing under the SEM. This improves the electron transmission of the samples and thus the contrast of the images obtained.

3.2.8 Fourier Transformed Infrared Spectroscopy (FTIR)

FTIR is used to determine the chemical composition of the obtained microparticles. In brief, dried samples were dissolved in dichloromethane and a drop of this solution was placed on NaCl

discs. FTIR spectra were recorded in the transmission mode using a Thermo FT-IR Nicolet-6700. The spectrum was taken from 4000 to 500 cm^{-1}.

3.2.9 Synthesis of PNIPAAm-AH copolymer

PNIPAAm-AH copolymer was prepared and analyzed to determine the LCST of the PNIPAAm-AH shell of MLMPs. The polymerization of poly (N-isopropylacrylamide-co-allylamine) [36] was carried out in de-ionized water at room temperature using BIS as the cross-linking agent, SDS and APS and TEMED as a pair of redox initiators. In brief, 0.75 g of NIPA, 0.143 g of AAm, 750 µL of AH, and 0.0262 g of BIS were dissolved in 100 mL of de-ionized water. The solution was purged with Ar for 30 minutes. 0.078 g of APS and 101 µL of TEMED were added to the solution and the reaction was carried out at room temperature under Argon for 2 hours. After the reaction was completed, the polymeric solution was dialyzed against de-ionized water using 6-8 kDa molecular weight cut off for 3 days to remove un-reacted materials before analysis.

3.2.10 LCST Determination of PNIPAAm-AH copolymer

The LCST of PNIPAAm-AH copolymer was determined using an UV-Vis spectrophotometer coupled with a temperature controller as described elsewhere [70]. 200 µl of PNIPAAm-AH polymeric solution samples (n=4) were used for the experiment. The samples were heated from 22^{o}C to 41^{o}C. Absorbance was recorded at 500 nm wavelength at several temperatures. The absorbance values were then converted into percentage of transmittance and a graph of

percentage of transmittance versus temperature was plotted. The LCST of PNIPAAm-AH copolymer was also determined by differential scanning calorimetry (DSC). The DSC measurements were carried out using a differential scanning calorimeter (Perkin-Elmer 7 series, DSC 7). The polymer was placed in aluminum hermetic sealed pans and the nanoparticle solution was heated at a rate of 1°C/min. A graph, heat flow versus temperature, was generated by DSC. The peak in the curve represents the LCST of the polymer.

3.2.11 Conjugation

In order to test our nanoparticles for future bioconjugation, either green fluorescent poly ethylene glycol with carboxylic activated group (PEG), or IgG conjugated to Texas Red was used as a conjugated biomolecule model. In order to conjugate PEG onto nanoparticles, 0.01 g of MLMPs were dissolved in 0.5 ml of MES (0.1 M) buffer solution and 0.01 g of EDC was added. The reaction was mixed for 10 minutes at room temperature. 0.2 mg of Fluor-PEG-SCM (FPS) was added to the above solution and the reaction was stirred vigorously for 24 hours at room temperature under dark conditions. The solution was dialyzed (MWCO 100 kDa) under dark conditions against DI-H2O for 1 week to remove un-reacted FPS. The sample was lyophilized and re-suspended in 50% glycerol in water before imaging.

In order to test the conjugation capability of the MLMPs, Texas Red IgG-TR (bovine anti-rabbit IgG-Texas Red) was also used. In brief, 0.01 g of MLMPs were dissolved in 0.5 ml of MES (0.1 M) buffer solution and 0.01 g of EDC was added. The reaction was mixed well for 10 minutes at room temperature. 0.2 mg of IgG-TR was added to the above solution and the reaction was stirred vigorously for 2 hours at room temperature under dark conditions. The solution was

dialyzed (MWCO 100 kDa) under dark conditions against DI-H2O for 1 week to remove un-reacted IgG-TR. The sample was lyophilized and re-suspended in 50% glycerol in water before imaging by an enhanced optical fluorescent microscope (Cytoviva).

3.2.12 Protein loading and release studies

The protein release behavior of biodegradable PLGA core alone, Thermo sensitive PNIPAAm-AH shell alone and the dual release behavior of the MLMP was determined using bovine serum albumin (BSA) as model protein for individual core and shell release. Whereas, BSA and flourescein disodium salt (FDS) are used as model proteins for duel protein delivery.

For evaluating the release of protein by PLGA microparticles, BSA loaded PLGA microparticles were prepared using a double emulsion solvent evaporation method. Loading efficiency of the particles was calculated indirectly where the amount of drug left in the supernatant after removing the drug-loaded particles was determined. This amount was subtracted from the initial concentration of drug to get the percentage loading efficiency (equation 1).

$$\text{Percentage loading efficiency} = \frac{(\text{Original conc} - \text{Supernatant conc})}{\text{Original conc}} \times 100 \qquad (1)$$

To study the amount of protein released at a certain time, the drug loaded particles were suspended in a known amount of PBS. Samples are dialyzed at 37ºC, and the dialysate was collected and replaced by fresh PBS at regular intervals of time up to a maximum of 4 weeks.

The collected samples were stored at -20ºC until analysis. The samples were analyzed for BSA release amount using BCA^{TM} protein assays (Pierce) following the manufacturer's instructions.

To determine the protein release behavior of MLMPs core, MLMPs were prepared with BSA loaded PLGA core and no drug/protein was loaded into the shell. Loading efficiency of the particles was calculated as mentioned above. These particles were then suspended in a known amount of PBS. Samples were dialyzed at 25ºC and 37ºC respectively, and the dialysate was collected and replaced by fresh PBS at regular intervals of time up to a maximum of 4 weeks. The collected samples were stored at -20ºC until analysis. The samples were analyzed for BSA release amount using BCA^{TM} protein assays (Pierce) following the manufacturer's instructions.

To determine the protein release behavior of MLMPs shell, MLMPs were prepared as mentioned earlier using non drug loaded PLGA microparticles. The shell of the microparticles was loaded with hydrophilic model protein BSA. In brief, BSA (30mg) was first loaded into MLMPs (60 mg) that were suspended in 20ml DI water. The solution was left on a shaker for 3 days at 4ºC to let the drug absorb into the shell of particles. The loading efficiency of the particles was determined using indirect method as described earlier by calculating the amount of BSA left in the supernatant after the particles were separated. Protein release behavior of these particles was determined at 25ºC and 37ºC temperatures as mentioned earlier. The samples collected were stored at -20ºC until analysis. The samples were analyzed for BSA release amount using BCA^{TM} protein assays.

Dual protein release behavior of MLMP was determined by using BSA and FDS as hydrophilic model drugs. MLMPs were prepared using BSA loaded PLGA microparticles as the core and

the shell of MLMPs were then loaded with FDS through drug absorption as mentioned earlier. The drug release behavior of these particles was determined using dialysis method at 25ºC and 37ºC temperatures. The samples were collected and stored at -20ºC until analysis. The samples were analyzed for BSA release amount using BCA^{TM} protein assays (Pierce) following the manufacturer's instructions. The amount of FDS presented in the samples was determined using fluoro-spectrophotometry with an excitation wavelength of 480nm and emission wavelength of 515nm (UV-Vis Spectrophotometer, Icontrol, M200). These readings were then compared with a standard curve (or known standards) to obtain the amount of FDS released.

3.2.13 3T3 fibroblast cell (FCs) culture

FCs (NIH) were cultured in complete medium consisting of Dulbecco's Modified Eagle Medium (DMEM) supplemented with 10% fetal bovine serum (FBS) and 1% penicillin-streptomycin. Cells were incubated in a humid environment at 37°C and 5% CO_2. Upon 80-90% confluence, the cells were passaged or used for experiments. Cells up to passage P12 were used in the experiments.

3.2.14 Cell adhesion and growth on PNIPAAm-AH surface

To determine the ability of the MLMPs surface to support cell adhesion and growth, glass slides were coated with PNIPAAm-AH copolymer through polymer deposition method. These glass slides were then seeded with FCs with a seeding density of 10000 cells/cm^2. The samples were

then incubated at 37ºC for 48 hours in the presence of complete growth media to allow cell adhesion and growth. After incubation samples were fixed with 2% paraformaldehyde, washed and dehydrated using 70%, 90% and 100% ethanol respectively. The samples were then freeze dried and observed under SEM (Hitachi, N3000).

3.2.15 Fibroblast cell isolation using MLMPs

Cell isolation studies were performed in order to determine the ability of the MLMPs to pick up cells in suspension. FCs were cultured using growth media as mentioned above. 10mg of MLMPs were weighed out sterilized and suspended in 1ml growth media through sonication. The cultured cells were then collected and suspended in a cell suspension flask (TPP, Bioreactor 50ml) along with particle suspension. The suspension flask is then left for incubation at 37ºC for 18 hours to allow cell adhesion and growth on the microparticles. After incubation particles were extracted using a magnet, washed with PBS and fixed using 2% paraformaldehyde solution. The samples were then observed under microscope and SEM to determine cell adhesion onto the microparticles.

3.2.16 Effect of MLMP cell isolation on cell morphology and growth

Studies were done to determine the effect of cell isolation on cell morphology and growth. Here, MLMPs were used to isolate FCs as mentioned above. The particles were extracted using magnet and washed with PBS to remove any cells not attached to the particles. The samples were then left for 30 minutes at room temperature in the growth media to allow cell detachment

from microparticles. This cell suspension was added to the glass slide and incubated at 37ºC for 24 hours to allow cell adhesion and growth back onto the glass slide. The cells were then fixed with 2% paraformaldehyde solution and stained using Hemotoxylyne and Eosin which stains cell nucleus and membrane respectively. The samples were then observed under microscope to determine cell morphology.

3.3 Results and Discussion

3.3.1 Size and morphological characterization of the microparticles

PLGA and MLMPs were observed using an SEM to determine the size and morphology of the particles. As seen in Figure 3.4(a) PLGA microparticles obtained were spherical in shape with size varying from 50 to 100µm. The particles were distributed uniformly and have smooth surface (inset of Figure 3.4(a)). As seen in Figure 3.3(b) the MLNP have a solid spherical morphology with a non-uniform rough surface, due to the presence of PNIPAAm-AH coated magnetic nanoparticles on the PLGA core. It is evident from the images that the SNMNP have been effectively coated onto the surface of PLGA microspheres. Also, as seen in the inset of Figure 3.4(b), SNMNPs are distributed uniformly throughout the surface of the PLGA core providing a nanotopography which improves the adhesion of the cells onto the microparticle surfaces.

3.3.2 Chemical composition of the microparticles

Even though the SEM pictures show the presence of the SNMNPS on the surface of the PLGA core, it does not prove the presence of PNIPAAm-AH coating on the SNMNPs layer. The

presence of PNIPAAm-AH copolymeric shell and consequently the formation of the desired MLMPs can be proved by determining the chemical composition of the microparticle.

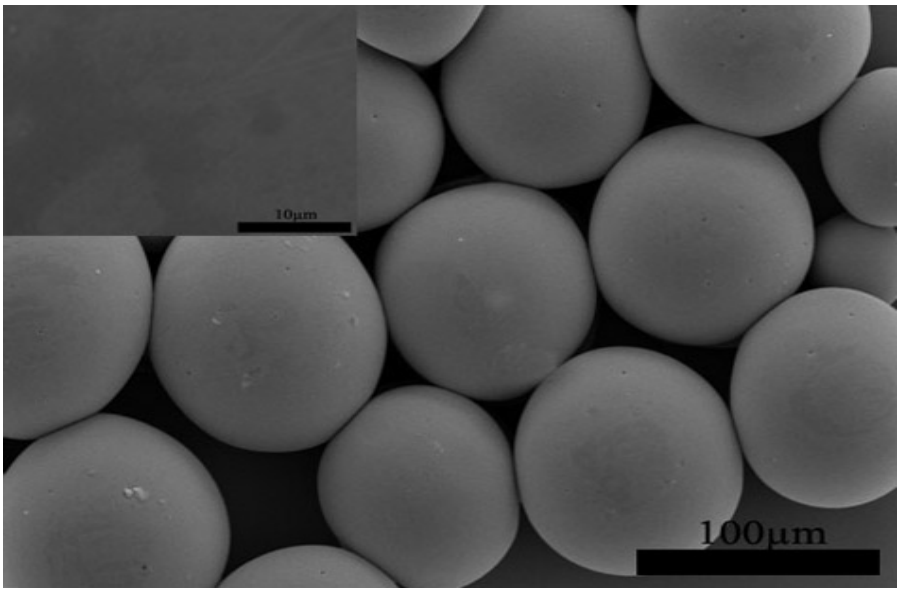

(a)

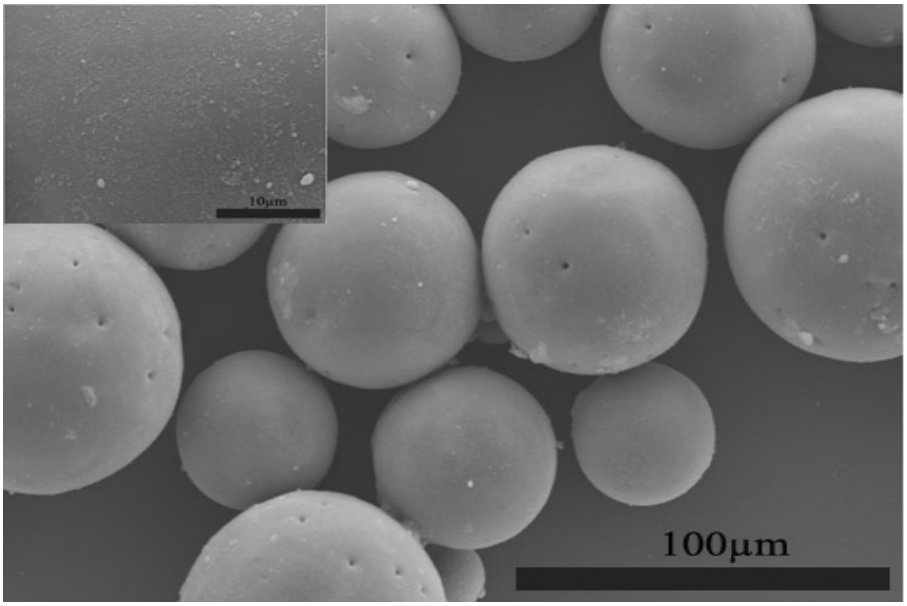

(b)

Figure 3.4: a) SEM image of PLGA microparticles b) SEM image of multilayered microparticles

FTIR spectrum of MLMPs was obtained and compared with that of PLGA, and PLGA-SNMNPs to determine whether appropriate polymerization of PNIPAAm-AH has occurred onto the microparticle or the particles seen in SEM are just PLGA-SNMNPs without the PNIPAAm-AH polymeric shell. As seen in Figure 3.5(b) the strong peaks in the range of 700-800 cm^{-1} correspond to the stretching mode of vinyl double bond present on the surface of the SNMNPs.

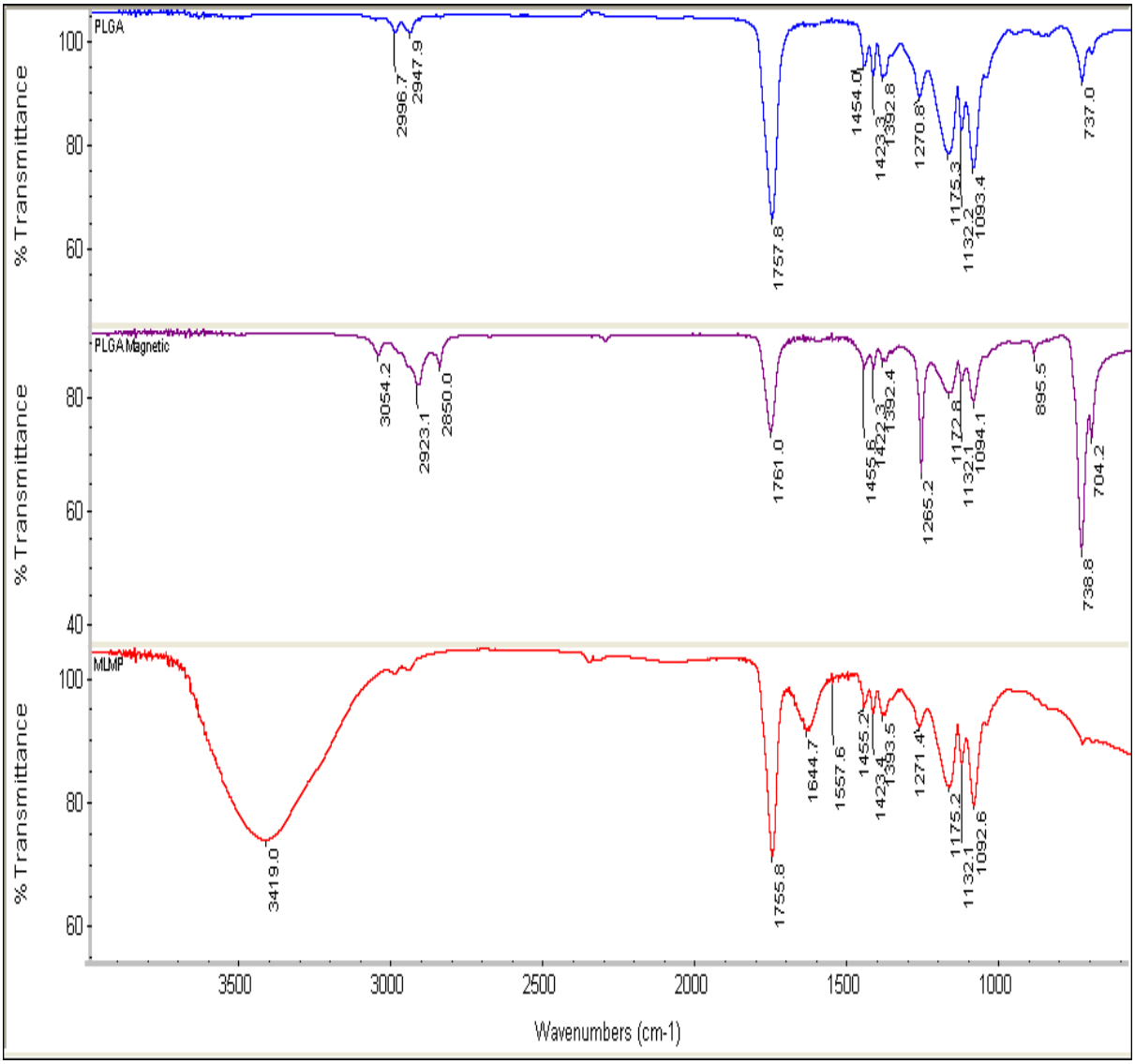

Figure 3.5: FTIR spectrum of a) PLGA, b) PLGA-SNMNPs and c) MLMPs

These vinyl bonds disappeared in the FTIR spectrum of MLMPs indicating the polymerization of NIPAAm-AH onto the SNMNPs layer. Also, the water attached in the process of polymer hydration and proton exchanged with the solvent give rise to a broad and intense peak at 3400cm^{-1} in MLMPs spectrum which are absent in the other spectrum. The –CH– stretching vibration of the polymer backbone is manifested through peaks at 2936-2969 cm^{-1}, while the two peaks in between 1600-1750 cm^{-1} correspond to the amide carbonyl group and the bending frequency of the amide N-H group respectively which confirms the presence of amine corresponding to the allylamine. From these observations it can be concluded that PNIPAAm-AH has been successfully coated onto the surface of the SNMNPs.

3.3.3 PNIPAAm-AH copolymer LCST determination

The LCST of the copolymer was observed around 34^{o}C. At temperatures below LCST, the polymeric solution is clearer; hence transmits more light and absorbs less. However, at temperatures above LCST, nanoparticle solution becomes cloudy due to change in confirmation of polymer becoming hydrophobic absorbs more light and transmits less.

In addition, DSC generated graph of heat flow versus temperature is seen in Figure 3.6. DSC analysis showed a detectable endothermic drop at 34.98°C which is close to the LCST by observation using spectrophotometry. Therefore, the LSCT of the polymer is between 34.5 - 35^{o}C and polymer is essentially hydrophilic under 34^{o}C where essential LCST transition occurs and the polymers becomes hydrophobic above 35^{o}C. Thus, the particles surface covered with

PNIAAm-AH copolymer is hydrophobic at incubation temperatures of 37ºC allowing cell adhesion and is hydrophilic at room temperature allowing cell detachment.

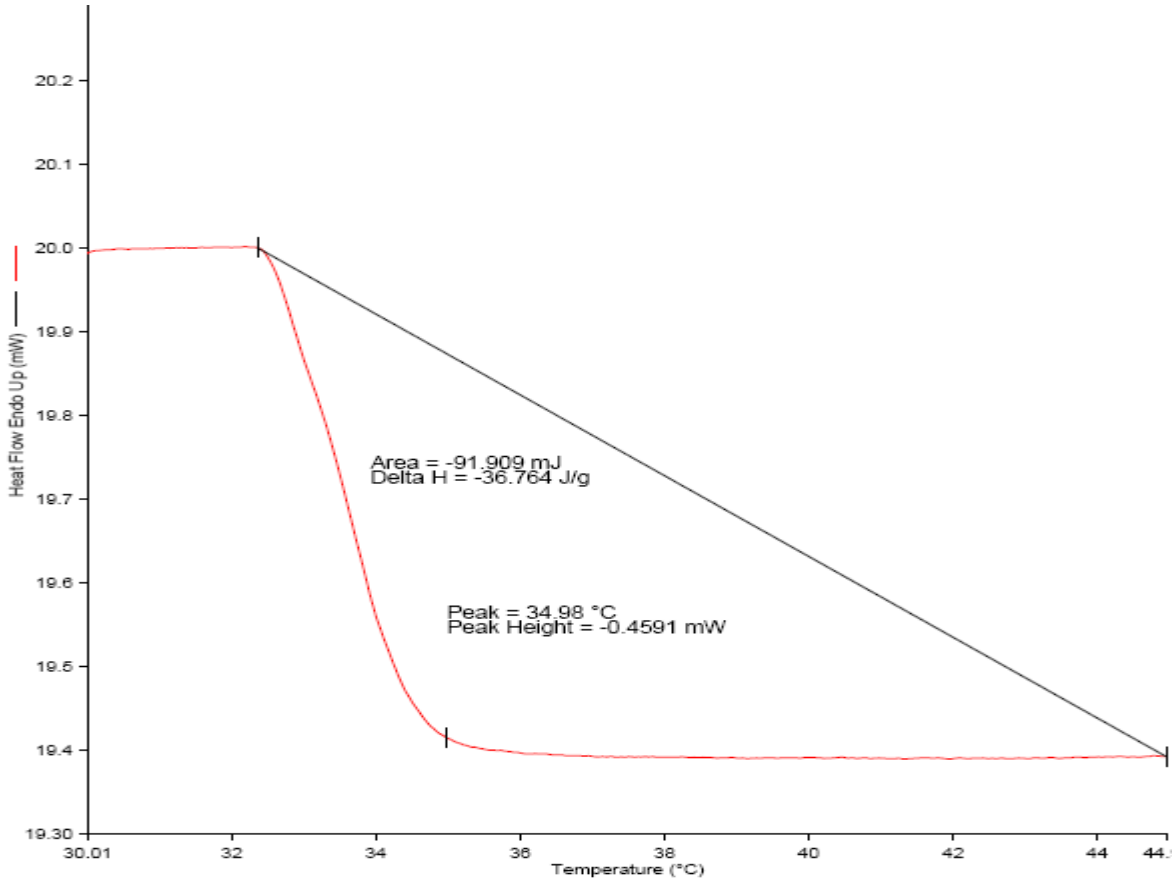

Figure 3.6: DSC endothermal heat flow graph showing the LSCT of PNIPAAm-AH copolymer

3.3.4 Conjugation studies

Conjugation studies were performed to access the capability of MLMPs to further conjugate with antibodies that are bound to particular cell types for cell isolation. MLMPs were essentially conjugated with fluorescent PEG (Green) and antibodies (Red) using carbodiimide chemistry. Conjugated particles were viewed under the cytoviva ™ fluorescent microscope. Figure 3.7

shows the MLMPs conjugated with florescent PEG. Bright green color is observed in fluorescent mode, whereas particles were almost transparent when seen in a phase contrast mode. Also, Figure 3.8 shows that MLMPs conjugated with fluorescent IgG were red in color when observed in florescent mode and were transparent in normal mode. These results indicate that florescent PEG and IgG were successfully conjugated onto the particles proving the presence of active amine functional groups on the surface of the microparticles. This functional group can be further used to conjugate with cell specific targeting moieties for specific cell isolation.

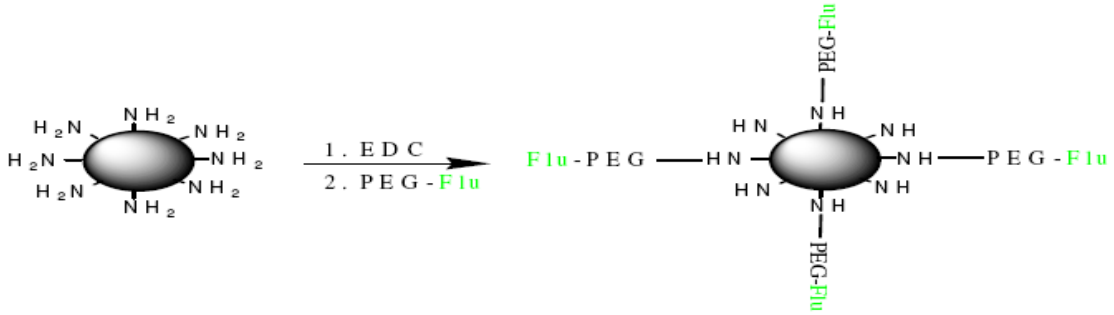

(a)

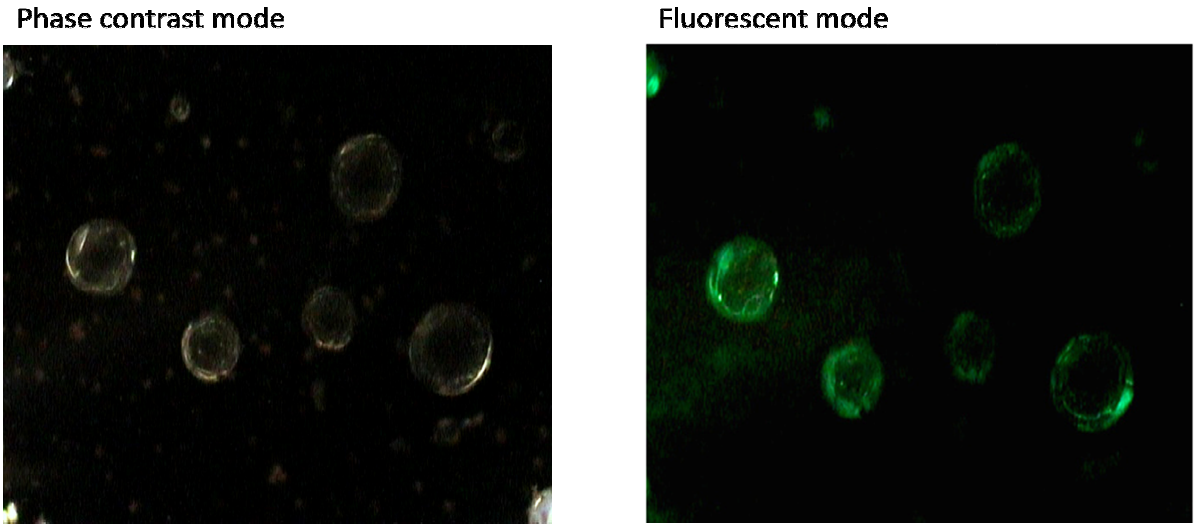

Figure 3.7: Conjugation of nanoparticles to fluorescent PEG. (a) Schematic diagram of the conjugation reaction of nanoparticles with Flu-PEG. (b) Fluorescent and phase contrast microscopy (cytoviva) image of MLMPs

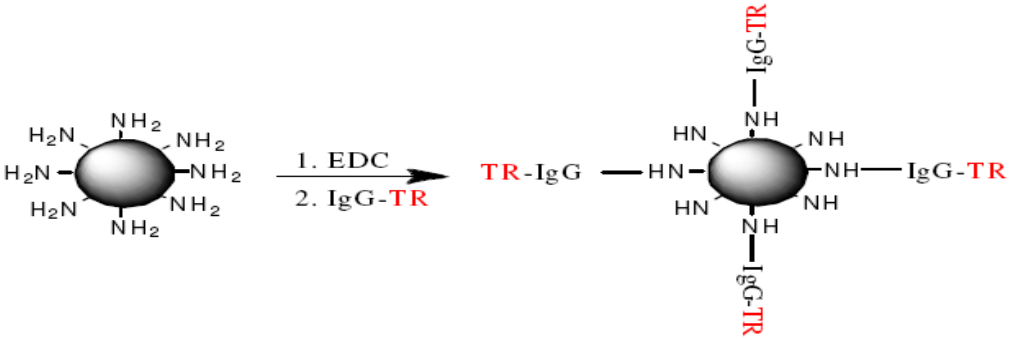

(a)

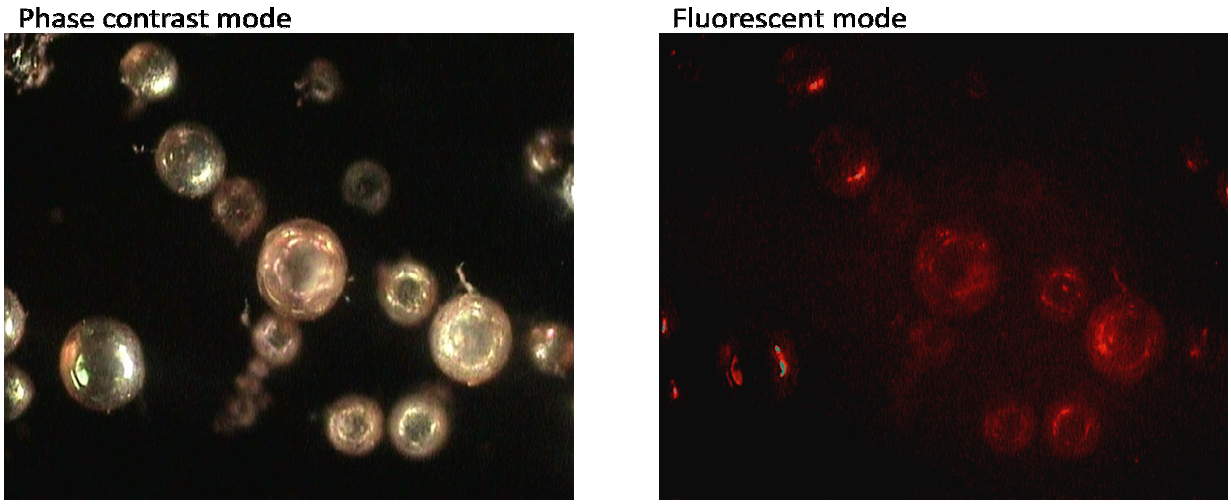

(b)

Figure 3.8: Conjugation of nanoparticles to fluorescent IGg. (a) Schematic diagram of the conjugation reaction of nanoparticles with Flu-IGg. (b) Fluorescent and phase contrast microscopy (cytoviva) image of MLMPs

3.3.5 Protein release profile of MLMPs

BSA is used as a model protein for core or shell alone release studies, whereas BSA and FDS are used for a dual protein release from both core and shell. These model hydrophilic components were selected for their ease of quantification. The loading efficiency of the particles was

calculated using indirect method as mentioned before. For MLMPs shell release studies the loading efficiency of MLMPs with protein loaded shell was 32% which was far less than previous studies (60-65%) where hydrophilic drug was loaded into PNIPAAm based nanoparticles [35, 36]. These were expected, given the effective area of microparticles is less than that of nanoparticles of same weight. Figure 3.9 (a) shows the release profile of MLMPs shell as different temperature (25 and 37ºC). The protein release was characterized by a burst release with most of protein releasing within 24 hours. Also, the release was dependent on the incubation temperature with more amount of loaded BSA being release at 37ºC (81%) than that at 25ºC (49%).

For core release studies the loading efficiency of BSA loaded in PLGA core was 55% which is consistent with other studies where PLGA is loaded with hydrophilic components [51, 52]. Figure 3.9 (b) shows the release profile of MLMPs core at 37ºC. The release was characterized by an initial burst release followed by a sustained release. The initial burst release might be due to the protein adsorbed on the particle surface being released followed by the protein release due to the degradation of the PLGA core and diffusing out of the PNIPAAm-AH shell. Also, only 50% of the total drug loaded was released which can be attributed to the protein being released during the MNP coating and PNIPAAm-AH polymerization process. Thus results indicate that protein release of core is dependent on both degradation of PLGA and the presence of polymeric shell.

Dual protein release studies were performed using BSA and FDS are model proteins to determine the effect of one drug release on the release of the other. The loading efficiency and release of the proteins (seen in Figure 3.10) were similar to that observed in protein release from

either core or shell alone. One important distinction is the lag phase observed in core BSA release followed by burst release (seen in Figure 3.10(b)). This might be because of the impedance caused by FDS loaded into the shell on BSA release. After 3 days most of the FDS is release thus prompting the sudden diffusion of BSA piled up during 3 days. Thus it can be concluded that the release of the shell is only dependent on temperature whereas, the release profile of core is dependent on PLGA degradation, and the diffusion through the shell.

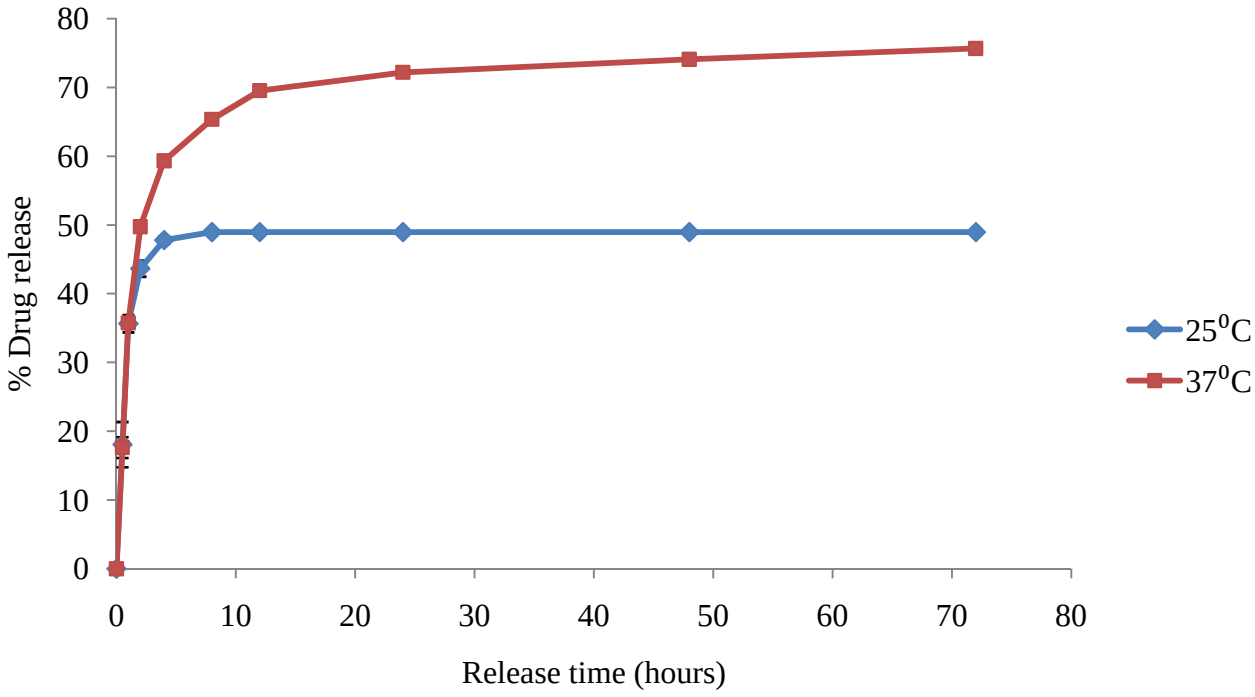

(a)

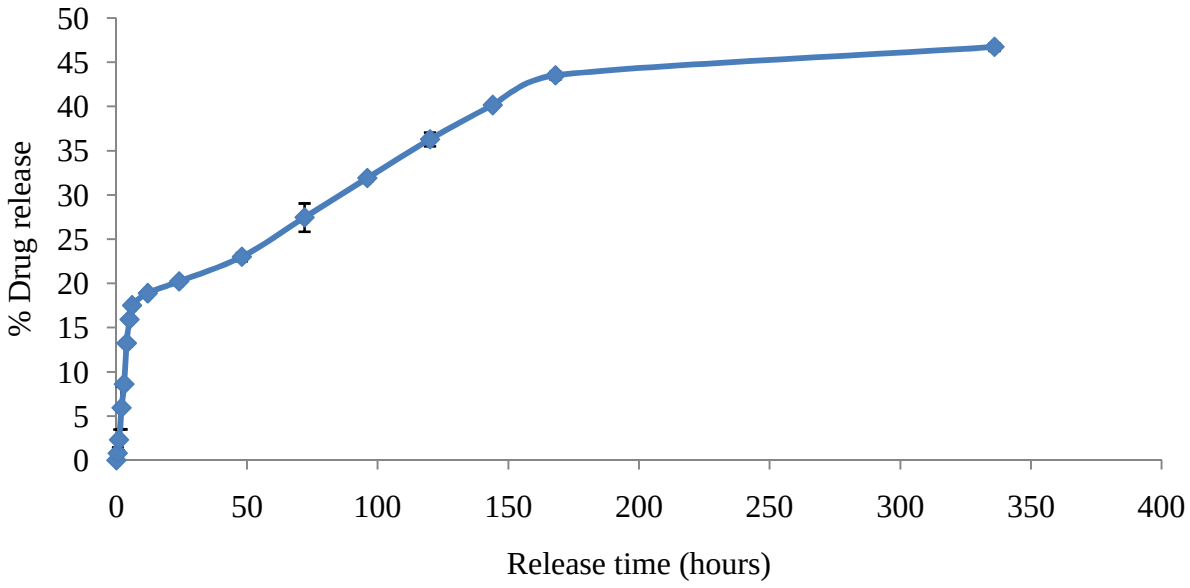

(b)

Figure 3.9: Release profiles of proteins from MLMPs core and shell (a) BSA release of MLMP shell alone (b) BSA release of MLMP core alone

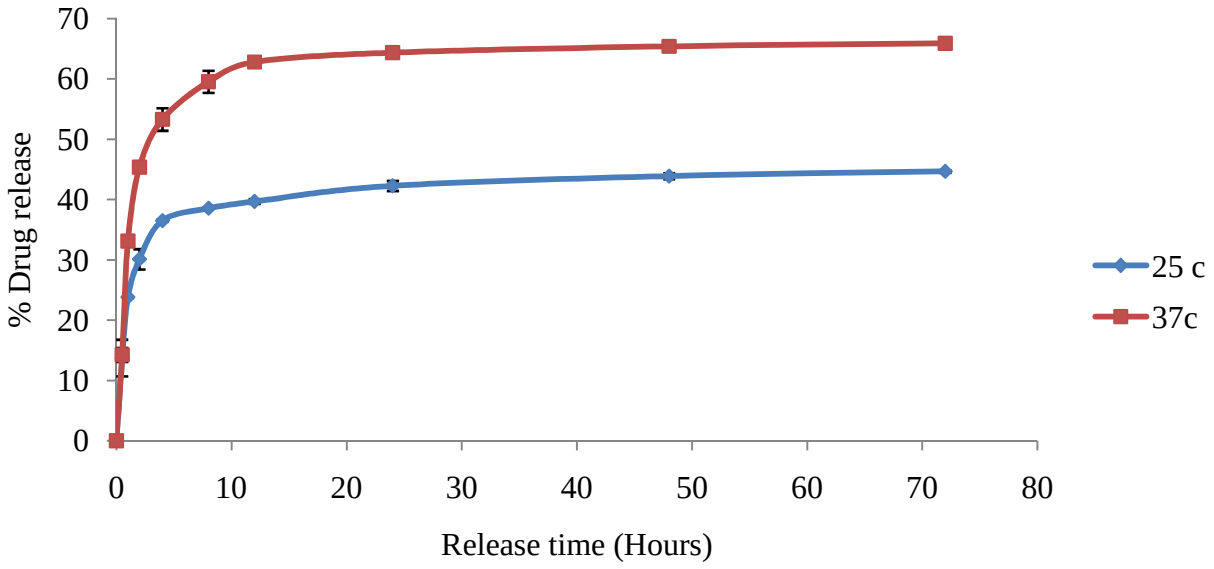

(a)

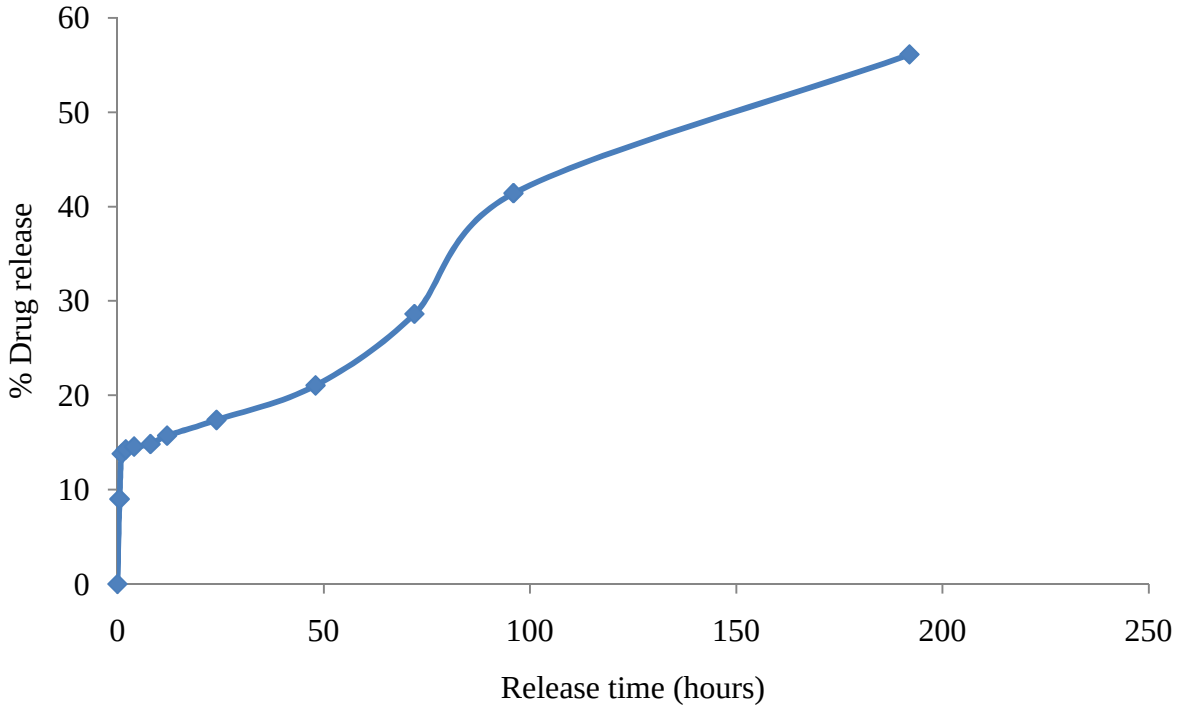

(b)

Figure 3.10: Dual protein release profile of MLMPs (a) Shell FDS release, (b) Core BSA release

3.3.6 Cell studies

The ability of the MLMPs surface to support cell adhesion was tested by growing FCs on PINIPAAm-AH coated glass slides. The slides were then observed under SEM to determine cell adhesion and morphology. As seen in Figure 3.11, cells were successfully attached to the polymer surface with a morphology characteristic to FCs. This indicates that the particle surface is hydrophobic at the incubation temperature of 37ºC and support cell adhesion and growth.

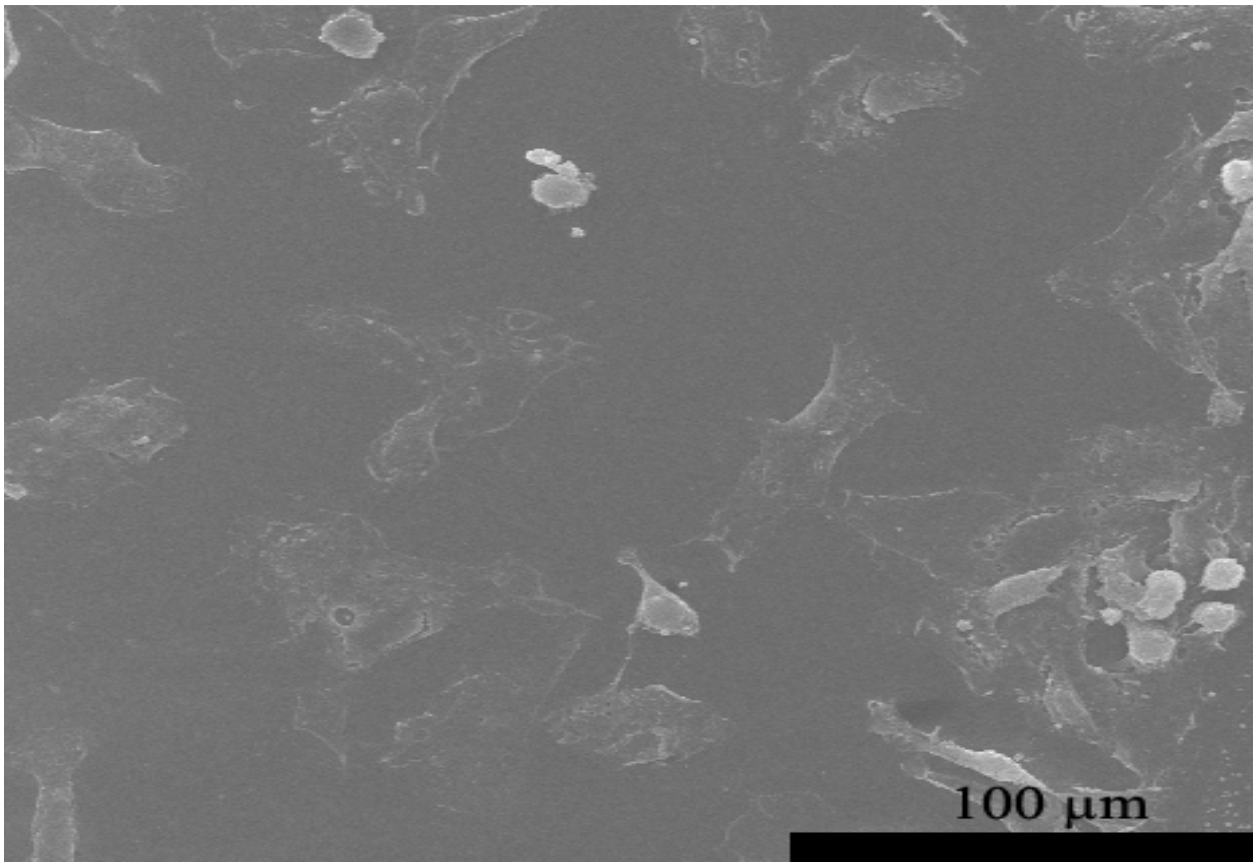

Figure 3.11: SEM image showing FCs attached onto PNIPAAm-AH coated glass slide

Also, to determine the ability of MLMPs to isolate cells from a suspension, FCs were extracted using MLMPs. MLMPs were incubated along with FCs in a suspension flask, and particles were then collected using an external magnet. These samples were then stained and observed under

cytoviva™. As seen in Figure 3.12 cytoviva™ images show cells clearly adhering to the surface of the microparticles, where consisting of green fluorescence and cells were stained red with membrane dye. From the image, cells have been attached to the particle surface and have been successfully isolated from suspension using an external magnet.

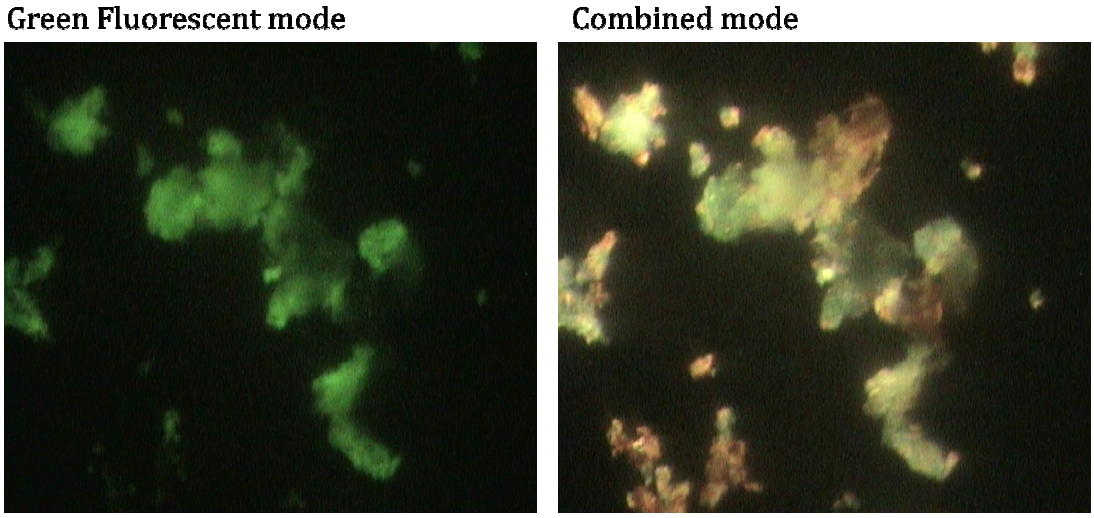

Figure 3.12: Cytoviva image showing FCs (Red) growing on the surface of the MLMP (Green)

Cells were isolated from the MLMP by exposure to room temperature as described earlier and cells were then reseeded onto a glass slide. Cells were grown for 24 hours and observed under microscope to determine the effect of cell isolation on cell morphology and growth. As seen in Figure 3.13 when compared to controls (FCs grown on a glass slide) isolated cells did not express any change in morphology. These results suggest that MLMPs can be used for successfully for cell isolation and have a minimal effect on cell viability.

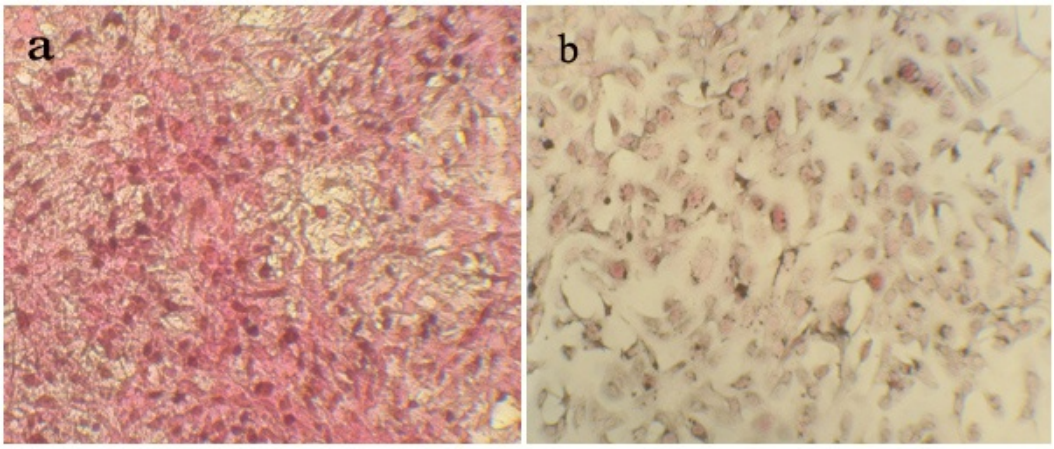

Figure 3.13: a) Conrol, b) FCs isolated by MLMP and reseeded onto a glass slide

3.4 Conclusion

In this study we have successfully developed multilayered microparticles with PLGA core and magnetic PNIPAAm-AH shell. SEM imaged showed that MLMPs of size 50-100µm were obtained with spherical morphology and rough surface. The presence of PNIPAAm-AH copolymeric shell was confirmed by FTIR. LCST studies showed that the shell had LSCT of 34-35ºC and the particles surface was hydrophobic above 35ºC and hydrophilic below 34ºC. Conjugation studies proved that the particles can further be conjugated with cell specific antibodies which can be used to isolating specific cells. Protein release studies showed that MLMPs can be loaded with two proteins. Protein release from shell was totally dependent on temperature with more protein being release at 37ºC, whereas protein release of core was dependent on PLGA degradation rate, diffusion of protein through polymeric shell, and impedance caused by protein loaded into the shell. Cell studies showed that the MLMPs surface promotes cell adhesion and growth and MLMPs can be used for isolating cells from suspension.

Also, cell isolation and detachment using MLMPs have a minimal effect on cell morphology and growth.

Experimental results show that MLMPs can be prepared and be used for cell isolation and enrichment. These particles have several advantages over conventional isolation procedures including that cells can be isolated without applying much chemical or physical strain. MLMP can also be loaded with proteins which can be used for cell enrichment and stem cell differentiation. Also, the isolated cells can be detached by just bringing down the temperature without any use of chemical such as trypsin as used by conventional cell detachment.

3.5 Limitations and Future work

MLMPs can be effectively used for cell isolation and have lot of advantages over conventional cell isolation procedures but, they are not perfect and have few limitations including PLGA degradation which disrupts MLMPs integrity rendering them unsuitable for long term cell culture. Also, conjugation of antibodies onto the surface of the surface of the particles may affect the targeting capabilities of the antibodies.

In the future MLMPs will be conjugated with cell specific antibodies and the effectiveness of the particles in isolating stem cells will be evaluated. Also, particles will be loaded with stem cell differentiating and enrichment factors and the effect of their release on cell differentiation and growth will be observed.

REFERENCES

1. Vogelson CT. (2001). Advances in Drug Delivery Systems. *Modern Drug Discovery*, 4(4): 49-52
2. J. Kreuter. Nanoparticles and microparticles for drug and vaccine delivery. *Journal of. Anatomy*, 189 (1996): 503 – 505
3. L. Brannon-Peppas. Recent advancements on the use of biodegradable microparticles and nanoparticles in controlled drug delivery. *International Journal of Pharmaceuticals*, 116 (1995): 1 – 9
4. Hanns J. W, Wolfgang E, Bernd M, and Heribert S.W. Tissue specific MR contrast agents. *European Journal of Radiology*, 46(1) (2003): 33-44
5. CH Reynolds, N Annan, K Beshah, JH Huber, S.H Shaber. Gadolinium-Loaded Nanoparticles: New Contrast Agents for Magnetic Resonance Imaging. *J. Am. Chem. So*,. 122 (37) (2000): 8940 -8945.
6. B.Bonnermail superparamagnetic agents in magnetic resonance imaging, physiochemical charecteristics and clinical applications. A review, *Journal of Drug \Target*, 6 (1998): 167 – 174
7. R. Weissleder, M. Papisov, Pharmaceutical iron oxides for MR Imaging, *Review of Magnetic Resonance Medicine*, 4(1992): 1-20
8. C. Claire, R. Philippe, I. Jean-marc, P Marc, Recent advances in iron oxide nanocrystal technology for medical imaging. *Science*, 58(2006): 1471-1504

9. J. Dobson, Gene therapy progress and prospects: magnetic nanoparticle-based *gene delivery*. *Gene Ther*, 13, (4) (2006): 283-287
10. A.K Gupta, S. Wells, Surface modified superparamagnetic nanoparticles for drug delivery: preparation, characterization, and cytotoxicity studies. *IEEE Trans Nanobioscience*, 3, (1) (2003): 66-73
11. Berry, C. C, Curtis A.S.G, Functonalisation of magnetic nanoparticles for applications in biomedicine. *Journal of Physics. D: Appllication Physics*, 36 (2003): 198 – 206
12. A. Ito, M. Shinka, H. Honda, T. Kobayashi, Medicalapplication of functionalized magnetic nanoparticles. *Journal of Bioscience and Bio engineering*, 100 (2005): 1 – 11
13. A. Jordan. Magnetic fluid hyprthermia (MFH): Cancer treatment with AC magnetic field induced excitation of biocompatible superparamagnetic nanoparticles. *Journal of Magnetism and Magnetic material*, 201 (1999): 413 – 419
14. F. Sonvico, S. Mornet, S. Vasseur, et al. Folate-conjugated iron oxide nanoparticles for solid tumor targeting as potential specific magnetic hyperthermia mediators: Synthesis, physicochemical characterization, and in vitro experiments. *Bioconjugate Chem*, 16 (2005): 1181 – 1188
15. I. Safarik, M. Safarikova. Use of magnetic techniques for the isolation of cells. *Journal of Chromatography B*, 722 (1999): 33 – 53
16. S. Miltenyi, W. Muller, W. Weichel, A. Radbruch. High gradient magnetic cell sepration with MACS. *Cytometry,* 11 (1990): 231 – 238.
17. A.H Lu, E. L Salabas, F. Schuth. Magnetic nanoparticles: synthesis, protection, functionalization, and application. *Angewandte Chemie (International ed),* 46 (8) (2007): 1222-1244

18. P. Gould. Nanomagnetism shows in vivo potential. *Nanotoday*, 1 (2006): 34 – 39
19. A. K Gupta, M. Gupta. Synthesis and surface engineering of iron oxide nanoparticles for biomedical applications. *Biomaterials*, 26 (18) (2005): 3995 – 4025
20. Seung-Jun Lee, Sung-Chul Shina, Jin-Chul Kimb, Young-Hwan Changa, Yong-Min Changc and J.-D.Jong-Duk Kim. Nanoparticles of magnetic ferric oxides encapsulated with poly(D,L latide-co-glycolide) and their applications to magnetic resonance imaging contrast agent. *Journal of Magnetism and Magnetic Materials*, (2004): 272-276
21. P. Grodzinski, M. Silver, L.K Molnar. Nanotechnology for cancer diagnostics: promises and challenges. *Expert review of molecular diagnostics*, 6 (3) (2006): 307 – 318
22. A. Pich, S. Bhattacharya, Y. Lu, V. Boyko, A.J Adler, Temperaturesensitive hybrid microgels with magnetic properties. *Langmuir: the ACS Journal of surfaces and Colloid*, 20 (24) (2004): 10706-10711
23. F. Eeckman F, A. J Moës, and K. Amighi. Synthesis and Characterization of Thermosensitive Copolymers for Oral Controlled Drug Delivery. *European Polymer Journal*, 40(4) (2004): 873-881
24. L. Yan, Q. Zhu, and P. U Kenkare. Lower Critical Solution Temperature of Linear PNIPA Obtained from a Yukawa Potential of Polymer Chains. *Journal of Applied Polymer Science*, 78(11) (2000): 1971-1976
25. M. Heskins and J. E Guillet. Solution Properties of Poly (*N*-isopropylacrylamide). *Journal of Macromolecular Science A: Pure & Applied Chemistry*, 2(8) (1968): 1441-1455
26. A.S Hoffman. Hydrogels for biomedical applications. *Annals of the New York Academy of Sciences*, 944 (2001): 62-73

27. Morimoto, N.; Endo, T.; Iwasaki, Y.; Akiyoshi, K., Design of hybrid hydrogels with self-assembled nanogels as cross-linkers: interaction with proteins and chaperone like activity. *Biomacromolecules,* 6 (4), (2005): 1829-1834
28. S.V Vinogradov, T.K Bronich, A.V Kabanov, Nanosized cationic hydrogels for drug delivery: preparation, properties and interactions with cells. *Advanced drug delivery review,*. 54 (1), (2002): 135-47
29. R.M Ramanan, P. Chellamuthu, L. Tang, K.T Nguyen, Development of a temperature-sensitive composite hydrogel for drug delivery applications. *Biotechnology Progress*. 22 (1), (2006): 118-125
30. Yamada N, Okano T, Sakai H, Karikusa F, Sawasaki Y, and Sakurai Y. Thermoresponsive Polymeric Surfaces; Control of Attachment and Detachment of Cultured Cells. *Die Makromolekulare Chemie, Rapid Communications*, 11(11) (1990): 570-576
31. Kushida A, Yamato M, Konno C, Kikuchi A, Sakurai Y, and Okano T. Decrease in Culture Temperature Releases Monolayer Endothelial Cell Sheets together with Deposited Fibronectin Matrix from Temperature-Responsive Culture Surfaces. *Journal of Biomedical Materials Research Part A*, 45(4) (1999): 355-362
32. Okano T, Yamada N, Okuhara M, Sakai H, and Sakurai Y. (1995). "Mechanism of Cell Detachment from Temperature-Modulated, Hydrophilic-Hydrophobic Polymer Surfaces." Biomaterials, 16(4): 297-303.
33. Canavan HE, Cheng X, Graham DJ, Ratner BD, and Castner DG. Cell Sheet Detachment Affects the Extracellular Matrix: A Surface Science Study Comparing Thermal Liftoff,

Enzymatic, and Mechanical Methods. *Journal of Biomedical Materials Research Part A,* 75A (1) (2005): 1-13

34. Lu AH, Salabas EL, Schuth F. Magnetic nanoparticles: synthesis, protection, functionalization, and application. *Angewandte Chemie (International ed),* 46(8) (2001):1222-1244
35. Maham Rahimi, Eftathios I. Meletis, Shaoxin You, and Kytai Nguyen. Formulation and Charecterization of Novel Temperature Sensitive Polymeric Coated Magnetic Nanoparticle. (2008):In press
36. Rahimi M, Yousef M, Cheng Y, Meletis EI, Eberhart RC. Formulation and Characterization of Covalently Coated Magnetic Nanogel. *Journal of Nanoscience and Nanotechnology*, (2008): in press
37. Brannon-Peppas L, Blanchette JO. Nanoparticle and targeted systems for cancer therapy. *Advanced drug delivery reviews,* 56(11) (2004): 1649-1659
38. C.X. Song , V. Labhasetwar , H. Murphy , X. Qu , W.R. Humphrey , R.J. Shebuski ,, Levya RJ. Formulation and characterization of biodegradable nanoparticles for intravascular local drug delivery. *Journal of Controlled Release,* 43 (1994): 197-212
39. Seung-Jun Leea J-RJACI, Sung-Chul Shina, Jin-Chul Kimb, Young-Hwan Changa, Yong-Min Changc and J.-D.Jong-Duk Kim. Nanoparticles of magnetic ferric oxides encapsulated with poly(D,L latide-co-glycolide) and their applications to magnetic resonance imaging contrast agent. *Journal of Magnetism and Magnetic Materials,* 272-276 (2004): 2432-2433
40. Sahoo SK, Labhasetwar V. Nanotech approaches to drug delivery and imaging. *Drug discovery today,* 15(24) (2003): 1112-1120

41. Lu AH, Salabas EL, Schuth F. Magnetic nanoparticles: synthesis, protection, functionalization, and application. *Angewandte Chemie (International ed)*, 46(8) (2007): 1222-1244
42. Adam CB. Functionalization of magnetic nanoparticles for applications in biomedicine. *Journal of Physics D: Applied Physics*, 36 (2003): 198 – 206
43. Cunningham CH, Arai T, Yang PC, McConnell MV, Pauly JM, Conolly SM. Positive contrast magnetic resonance imaging of cells labeled with magnetic nanoparticles. *Magnetic Resonance Medicine*, 53(5) (2005): 999-1005
44. Seung-Jun Leea J-RJACI, E-mail The Corresponding Author, a, Sung-Chul Shina, Jin-Chul Kimb, Young-Hwan Changa, Yong-Min Changc and J.-D.Jong-Duk Kim. Nanoparticles of magnetic ferric oxides encapsulated with poly(D,L latide-co-glycolide) and their applications to magnetic resonance imaging contrast agent. *Journal of Magnetism and Magnetic Materials*, (2004): 272-276:2432-2433
45. Grimal JM MP. The anodic dissolution and passivation of Ni-Cr-Fe alloys studied by ESCA. *Corrosion Science*, 33 (1995): 805-814
46. Zhu KJ, Jiang HL, Du XY, Wang J, Xu WX, Liu SF. Preparation and characterization of hCG-loaded polylactide or poly(lactide-co-glycolide) microspheres using a modified water-in-oil-in-water (w/o/w) emulsion solvent evaporation technique. *Journal of microencapsulation*, 18(2) (2001): 247-260
47. Jong Ryul Jeong, Seung Jun Lee, Jong Duk Kim, and Sung Chul Shin. Magnetic properties of Fe3O4 nanoparticles encapsulated with poly(D, L Lactide-Co-Glycolide). *IEEE Transactions on Magnetics*, 40(4) (2004): 3015-3017

48. Gupta AK, Gupta M. Cytotoxicity suppression and cellular uptake enhancement of surface modified magnetic nanoparticles. *Biomaterials,* 226(13) (2005): 1565-1573

49. M. Chacon, L. Berges, J. Molpeceres, M.R. Aberturas, M. Guzman. Optimized preparation of poly D,L (lactic-glycolic) microspheres and nanoparticles for oral administration. *International Journal of Pharmaceutics,* 141 (1996): 81-91

50. Yilmaz Capan BHW, Sisay Gebrekidan, Shamim Ahmed and Patrick P. DeLuca. Influence of formulation parameters on the characteristics of poly(Image -lactide-co-glycolide) microspheres containing poly(Image -lysine) complexed plasmid DNA. *Journal of Controlled Release,* 60(2-3) (1999): 279-286

51. P. D. Scholes, A. G. A. Coombes, L. Illum, S. S. Daviz, M. Vert and M. C. Davies. The preparation of sub-200 nm poly(lactide-co-glycolide) microspheres for site-specific drug delivery. *Journal of Controlled Release,* 25(1-2) (1993):145-153

52. Mu L, Feng SS. A novel controlled release formulation for the anticancer drug paclitaxel (Taxol): PLGA nanoparticles containing vitamin E TPGS. *Journal of Control Release*, 86(1) (2003): 33-48

53. Ugelstad J, Olsvik O, Schmid R, Berge A, Funderud S, Nustad K. Molecular interactions in Bio-separations. *Plenum press, Newyork,* (1993) 229-235

54. Prestvik W.S, Berge A, Mork P.C, Stenstad P.M, and Ugelstad J. Scientific and clinical applications of magnetic carriers. *Plenum press, Newyork,* (1997): 11-16

55. Safarik I, Safarikova M, Forsythe SJ. The application of magnetic separations in applied microbiology. *Journal of Application Bacteriology,* 78 (6) (1995): 575-585

56. Olsvik O, Popvic T, Skjerve E, Cudjoe K.S et al. Magnetic separation techniques in diagnostic microbiology. *Clinical Microbiology Review,* 7(1) (1994): 43-54

57. Owen C.S. Magnetic cell sorting using collodial protein magnetite. *International Journal of Immunogenetics,* 16(2) (2007): 117-123

58. Rey P.D. Sweet and sticky: Carbohydrate coated magnetic beads. *Biotechnology,* 14 (1996): 155-157

59. Chalmers J.J, Zborowski Maciej, Sun L. Flow through immunomagnetic cell separation. *Biotechnology Progress,* 14 (1998): 141-18

60. Jeffery H, Davis S. S, Ohagan D. T. The preparation and characterisation of poly(lactide-co-glycolide) microparticles. I : Oil-in-water emulsion solvent evaporation. *International Journal of Pharmaceuticals,* 77(2-3) (1997): 169-175

61. Rajeev A.J. The manufacturing techniques of various drug loaded biodegradable poly(lactide-*co*-glycolide) (PLGA) devices. *Biomaterials,* 21 (23) (2000): 2475-2490

62. Yamaguchi Y, Takenaga M, Kitagawa Y, Ogawa Y, Mizushima Y, and Igarashi R. Insulin loaded biodegradable PLGA microcpsules: Initial burst release controlled by hydrophilic additives. *Journal of Controlled Release,* 81 (3) (2002): 235-249

63. Anne A.P, Marie-Claire V.J, Patrick S, Michelle S, Jean-Pierre B. Preparation of PLGA microparticles by an emulsion extraction process using glycofurol as polymer solvent. *Pharmaceutical Research,* 21 (12) (2004): 2384-2391

64. Wu, X. S., Wang, N. Synthesis, characterization, biodegradation, and drug delivery application of biodegradable lactic/glycolic acid polymers. Part II: biodegradation. *Journal of biomaterials science. Polymer edition,* 12(1) (2001): 21-34.

65. Patrick B, O'Donnell and James W.M. Preparation of microspheres by the solvent evaporation technique. *Advanced Drug Delivery Reviews,* 28 (1) (1997): 25-42

66. Wakamatsu H, Yamamoto K, Nakao A, Aoyagi T. Preparation and characterization of temperature responsive magnetite nanoparticles conjugated with Nisopropylacrylamide-based functional copolymer. *Journal of Magnetization and Magnetization Materials,* 302 (2) (2006): 327-333.

67. Beuermann S, Buback M, Hesse P, Hutchinson R. A, Kukučkova S, Lacik I. Termination Kinetics of the free-radical polymerization of nonionized methacrylic acid in aqueous solution. *Macromolecules*, 2008**:** In press.

68. Wang, P. C.; Chiu, W. Y.; Lee, C. F.; Young, T. H., Synthesis of iron oxide/poly (methyl methacrylate) composite latex particles: nucleation mechanism and morphology. *Journal of Polymer Science Part A: Polymer Chemistry*, 42 (2004): 5695-5705

69. Jon A.R, Gerard M, and David J.M. Aliginate hydrogels as synthetic extracelular matix materials. *Biomaterials*, 20 (1) (1999): 45-53

70. Fundueanu G, Constantin M, Bortolotti F, Ascenzi P, Cortesi R, and Menegatti E. Preparation and Characterisation of Thermoresponsive Poly[(*N*-isopropylacrylamide-co-acrylamide-co-(hydroxyethyl acrylate)] Microspheres as a Matrix for the Pulsed Release of Drugs. *Macromolecular Bioscience*, 5(10) (005): 955-964.

BIOGRAPHICAL INFORMATION

Bhanuprasanth Kopolu was born in the city of Nellore, Andhrapradesh, India in August 1984. He graduated with a Bachelor of Engineering degree in Biomedical Engineering from the Narayana Engineering College, Jawaharlal Nehru Technological University, Andhrapradesh, India in June 2006. He moved to the United States in December 2006 in pursue of higher studies. After enrolling in the Biomedical Engineering program at the University of Texas at Arlington, he began conducting research under the guidance of Dr. Kytai Nguyen. His research interests include drug delivery, biomaterials and tissue engineering. After completing the Master of Science degree in Biomedical Engineering, he intends to gain industrial experience before pursuing a Ph.D. degree in the same field.